"Modeling Heterogeneous Catalytic Reactions: From the Molecular Process to the Technical System"
O. Deutschmann (Ed.), Wiley-VCH, Weinberg (2011).

First-Principles Kinetic Monte Carlo Simulations for Heterogeneous Catalysis: Concepts, Status and Frontiers

Karsten Reuter
Fritz-Haber-Institut der Max-Planck-Gesellschaft, Faradayweg 4-6, D-14195 Berlin, Germany

I. INTRODUCTION

Forming the basis for the production of virtually all every-day products, catalysis has always been the driving force for chemical industries. In the 21st century, the concomitant importance of catalysis research is even further increased by the worldwide rapidly growing demand for more efficient exploitation of energy and materials resources. As in many other areas of materials science, modern computational science is becoming a key contributor in the quest to quantitatively understand the molecular-level mechanisms underlying the macroscopic phenomena in chemical processing, envisioned to ultimately enable a rational design of novel catalysts and improved production strategies. Of particular relevance are hierarchical approaches that link the insights that modeling and simulation can provide across all relevant length and time scales.[1] At the molecular level, first-principles electronic-structure calculations unravel the making and breaking of chemical bonds. At the mesoscopic scale, statistical simulations account for the interplay between all elementary processes involved in the catalytic cycle, and at the macroscopic scale continuum theories yield the effect of heat and mass transfer, ultimately scaling up to a plant-wide simulation.

A comprehensive control of catalytic processes requires to address all of these facets and will thus ultimately necessitate novel methodological approaches that integrate the various levels of theory into one multi-scale simulation. With the focus on the surface chemistry, first-principles kinetic Monte Carlo (kMC) simulations for heterogeneous catalysis represent precisely one step in this direction. A proper evaluation of the surface kinetics also dictates to unite two distinctly different aspects and in turn two distinct methodologies[2]: The first important part is an accurate description of the involved elementary steps, typically comprising adsorption and desorption processes of reactants and reaction intermediates, as well as surface diffusion and surface reactions. When aiming at a material-specific modeling that is at best of predictive quality, the computation of the corresponding kinetic parameters is the realm of electronic structure theories[3–5] that explicitly treat the electronic degrees of freedom and thus the quantum-mechanical nature of the chemical bond.

Even though such a set of first-principles kinetic parameters constitutes already an (even for the most simple model systems hitherto barely achieved) important intermediate goal and highly valuable result, it does not suffice for a description of the surface catalytic function. For this, a second key ingredient is the occurrence (and thus relevance) of the individual elementary processes, in particular of the different reaction mechanisms. An evaluation of this statistical interplay within the manifold of elementary processes obviously needs to go beyond a separate study of each microscopic process. Taking the interplay into account naturally necessitates the treatment of larger surface areas. Much more challenging than this size, however, is the fact that the surface catalytic system is of course "open" in the sense that reactants, reaction intermediates and products continuously impinge from and desorb into the surrounding gas phase. Due to the highly activated nature of many of the involved elementary steps, the correspondingly required evaluation of the chemical kinetics faces the problem of a so-called "rare-event dynamics", which means that the time between consecutive events can be orders of magnitude longer than the actual process time itself. Instead of the typical picosecond time scale on which say a surface diffusion event takes place, it may therefore be necessary to follow the time evolution of the system up to seconds and longer in order to arrive at meaningful conclusions concerning the statistical interplay.

Tackling such demanding simulation times is the objective of modern non-equilibrium statistical mechanics techniques, many of which rely on a master equation type description that coarse-grains the time evolution to the relevant rare-event dynamics.[6,7] Kinetic Monte Carlo simulations[8,9] fall within this category, and distinguish themselves from alternative approaches in that they explicitly consider the correlations, fluctuations and spatial distributions of the chemicals at the catalyst surface. For given gas-phase conditions, the typical output of such simulations are then the detailed surface composition and occurrence of each individual elementary process at any time. Since the latter comprises the surface reaction events, this also gives the catalytic activity in form of products per surface area, either time-resolved, e.g. during induction, or time-averaged during steady-state operation.

Summarized in one sentence the central idea of first-principles kMC simulations for heterogeneous catalysis is

thus to combine an accurate description of the elementary processes with an account for their statistical interplay in order to properly evaluate the surface chemical kinetics. As such, the approach is the result of a twofold choice: The choice to employ first-principles electronic structure calculations, presently predominantly density-functional theory (DFT), to obtain the kinetic parameters of the individual processes, and the choice to employ a master equation based kMC algorithm to tackle the required long simulation times. Aiming to give an introduction to this technique, the main purpose of the present Chapter is therefore to motivate in detail why such a combination of distinct theories is necessary at all, what can be expected from it, and to critically discuss its advantages and limitations in comparison to alternative approaches. I will try to achieve this goal by first going step by step through the underlying concepts, mostly illustrating the ideas with a simple toy system. Instead of aiming at the hopeless undertaking to give a comprehensive overview of existing applications in the field, a subsequent Section will then illustrate the use of first-principles kMC for catalysis-related problems focusing on one showcase. Emphasis is hereby placed on highlighting the capabilities of, but also the challenges to such modeling. This then provides a natural starting point for the last Section, in which I will sketch where I see the current frontiers of this technique – and it will become quite obvious that as always in cutting-edge research there is still "lots of room at the bottom".

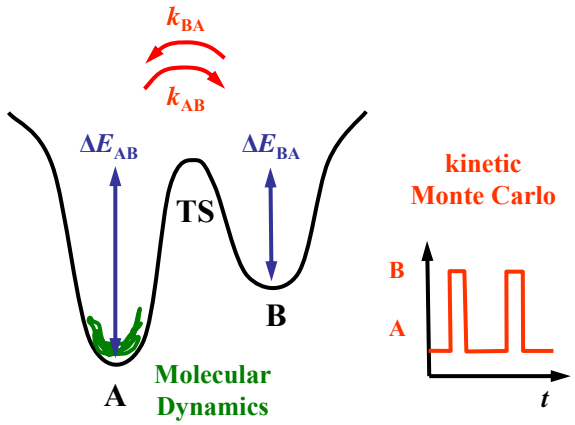

FIG. 1: Schematic representation of the relevant degree of freedom of the PES underlying the surface diffusion problem discussed in the text: Two stable adsorption sites A and B of different stability are separated by a sizable barrier. A MD simulation of this problem would explicitly follow the dynamics of the vibrations around either minimum and would therefore most likely never escape to the other basin within affordable simulation times. KMC simulations coarse-grain this short-time dynamics into the rate constants, k_{AB} and k_{BA}, and consider the discrete state-to-state dynamics as prescribed by a Markovian master equation. Transition-state theory (TST) is employed to derive the rate constants from the underlying PES, where in harmonic TST the barrier heights, ΔE_{AB} and ΔE_{BA}, as well as the vibrational modes at the minima and the transition state (TS) are required.

II. CONCEPTS AND METHODOLOGY

A. The problem of a rare-event dynamics

Instead of a more formal derivation, let me develop the more detailed conceptual discussion on the basis of a simple toy system. Consider the diffusive surface motion of an isolated atomic reaction intermediate that chemisorbs more or less strongly to specific sites offered by a solid surface. At finite temperature T the adsorbate will vibrate around its adsorption site with a frequency on the picosecond time scale, and diffuse (depending on its bond strength) say about every microsecond between two neighboring sites of different stability. The actual diffusion process itself takes thereby also only a picosecond or so, and in the long time in between the adsorbate does really nothing else than performing its random thermal vibrations. Obviously, if we want to get a proper understanding of what is going on in this system this requires us to follow its time evolution at least over a time span that includes several of the rare hops to neighboring sites, i.e. here of the order of several microseconds or more. Despite its simplicity, this toy model carries thus all the characteristics of a rare-event system, in which the relevant dynamics of interest (here the hops over the surface) proceeds by occasional transitions with long periods of time in between. This separation of time scales between thermal vibrations and the actual diffusion events results from the necessity to break (or "activate") chemical bonds in the latter. Highly activated processes are quite typical for surface chemistry and catalysis[10–12], and correspondingly such a rare-event dynamics is more the norm than an exception.

An important concept to further analyse the dynamics of our toy system is the so-called potential energy surface (PES).[13] While chemical bonds are the consequence of electronic interactions, a frequently justified approximation is to assume that the electron dynamics takes place on much faster time scales than the motion of the atomic nuclei. In this Born-Oppenheimer picture the electrons therefore adapt adiabatically to every configuration of atomic positions $\{\mathbf{R}_I\}$, and, reciprocally, the atoms can be viewed as traveling on the PES landscape $E\{\mathbf{R}_I\}$ established by the electronic interactions. The forces acting on a given atomic configuration are then the local gradient of the PES, and a (meta)stable atomic configuration corresponds to a (local) minimum of this landscape. In the language of a PES, the relevant degree of freedom of our surface diffusion problem can therefore schematically be described as shown in Fig. 1: Two neighboring adsorption sites of different stability are represented by two minima of different depths, separated by a sizable barrier as characteristic for the activated diffusion process.

A widely employed approach to follow the time evo-

lution at the atomic level are molecular dynamics (MD) simulations, which correspond to a numerical integration of Newton's equations of motion.[14] Starting in any one of the two minima and using the forces provided by the PES gradient, a MD trajectory would therefore explicitly track the entire thermal motion of the adsorbate. In order to accurately resolve the picosecond-scale vibrations around the PES minimum this requires time steps in the femtosecond range. Surmounting the high barrier to get from one basin to the other is only possible, if enough of the random thermal energy stored in all other degrees of freedom gets coincidentally united in just the right direction. If this happens as in our example only every microsecond or so, a MD simulation would have to first calculate of the order of 10^9 time steps until one of the really relevant diffusion events can be observed. Even if the computational cost to obtain the forces would be negligible (which as we will see below is certainly not the case for PESs coming from first-principles calculations), this is clearly not an efficient tool to study the long-term time evolution of such a rare-event system. In fact, such long MD simulations are presently computationally not feasible for any but the most simple model systems, and spending CPU time into any shorter MD trajectory would only yield insight into the vibrational properties of the system.

B. State-to-state dynamics and kMC trajectories

The limitations to a direct MD simulation of rare-event systems are therefore the long time spans, in which the system dwells in one of the PES basins before it escapes to another one. Precisely this feature can, however, also be seen as a virtue that enables a very efficient access to the system dynamics. Just because of the long time spent in one basin, it should not be a bad assumption that the system has forgotten how it actually got in there before it undergoes the next rare transition. In this case, each possible escape to another PES basin is then completely independent of the preceding basins visited, i.e. of the entire history of the system. With respect to the rare jumps between the basins, the system thus performs nothing but a simple Markov walk.[6]

Focusing on this Markovian state-to-state dynamics, i.e. coarse-graining the time evolution to the discrete rare events, is the central idea behind a kMC simulation. Methodologically, this is realized by moving to a stochastic description that focuses on the evolution with time t of the probability density function $P_i(t)$ to find the system in state i representing the corresponding PES basin i. This evolution is governed by a master equation, which in view of the just discussed system properties is of a simple Markovian form[6],

$$\frac{dP_i(t)}{dt} = -\sum_{j\neq i} k_{ij} P_i(t) + \sum_{j\neq i} k_{ji} P_j(t) \quad , \qquad (1)$$

where the sums run over all system states j. The equation thus merely states that the probability to find the system in a given state i at any moment in time t is reduced by the probabilities to jump out of the present state i into any other basin j, and is increased by the probabilities to jump from any other basin j into the present state i. These various probabilities are expressed in the form of rate constants k_{ij}, which give the average escape rate from basin i to basin j in units of inverse time. Because of the Markovian nature of the state-to-state dynamics, also these quantities are independent of the system history and thus an exclusive function of the properties of the two states involved. Assuming for now that all rate constants for each system state are known, the task of simulating the time evolution of the rare-event system is in this description then shifted to the task of solving the master equation, Eq. (1).

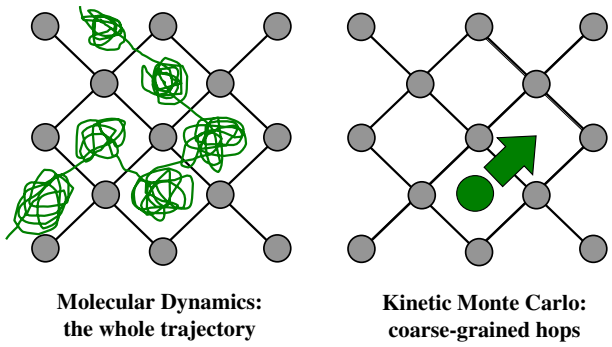

FIG. 2: Schematic top view explaining the differences between a MD (left panel) and a kMC (right panel) trajectory. Sketched is the path covered by an adsorbate that diffuses over the surface by rare hops to nearest-neighbor sites. Whereas the MD trajectory resolves the short-time vibrational dynamics around the stable adsorption sites explicitly, this is coarse-grained into the rate constants in the kMC simulations so that the corresponding trajectory consists of a sequence of discrete hops from site to site.

As we will see in the application example below, the typical number of states in models for a reactive surface chemistry is so huge that an analytic solution of the corresponding high-dimensional master equation is unfeasible. Following the usual stochastic approach of Monte Carlo methods[14,15], the idea of a kMC algorithm is instead to achieve a numerical solution to this master equation by generating an ensemble of trajectories, where each trajectory propagates the system correctly from state to state in the sense that the average over the entire ensemble of trajectories yields probability density functions $P_i(t)$ for all states i that fulfill Eq. (1).

Since this ensemble aspect of kMC trajectories is quite crucial, let me return to our example of the diffusing adsorbate to further illustrate this point. Figure 2 shows a schematic top view of our model surface sketching the path covered by the adsorbate in a time span covering a few of the rare diffusion events. The left panel shows the trajectory as it would have been obtained in a MD

simulation. The rare-event limitations to this simulation technique are obvious by the many wiggles around each one of the stable adsorption sites visited, representing the large time span of vibrational motion before the adsorbate achieves the rare transition to a neighboring site. The efficiency of a corresponding kMC trajectory, shown in the right panel of Fig. 2, results precisely from the fact that this vibrational short-term dynamics is eliminated from the simulation and (as we will see below) is instead appropriately accounted for in the rate constants k_{ij}. The trajectory consists therefore of a mere series of discrete hops from one stable adsorption site to another one, or in the language of the master equation from state i to another state j. Through which sequence of sites and at which transition times the kMC trajectory proceeds is randomly chosen by the kMC algorithm under appropriate consideration of the probabilities as contained in the rate constants k_{ij}. Contrary to the (for defined initial positions and momenta) deterministic MD trajectory, kMC trajectories are therefore only meaningful in the sense that averaging over a sufficiently large number of them yields the correct probability with which the system is in any of the states i at any moment in time t.

While this must always be kept in mind, it is also worth noticing that the computation of most quantities of interest would equally require some averaging over MD trajectories. If we take the diffusion coefficient as a typical target quantity within the area of our surface diffusion model, one possible approach to the involved computation of the average displacement per time would for example be to average over many hops observed during one sufficiently long MD trajectory or average over many shorter MD trajectories covering just one hop and starting with different initial momenta. As long as the Markov approximation is exactly fulfilled and the rate constants are accurate, the result obtained from an averaging over different kMC trajectories and the result obtained from the MD procedure would then be indistinguishable, only that the kMC approach is vastly more efficient and thus presumably the only one of the two that is computationally tractable.

C. kMC algorithms: From basics to efficiency

A kMC trajectory consists of a sequence of discrete hops from one system state to another, where the random selection of which state is next visited and after which amount of time the corresponding hop occurs follows the probabilities prescribed by the master equation, Eq. (1). Starting in any given state of the system, an algorithm generating such a trajectory must therefore appropriately determine in which state to jump next and what the corresponding escape time $\Delta t_{\rm escape}$ is. The system clock is then advanced by the escape time, $t \to t + \Delta t_{\rm escape}$, and the procedure starts anew. As illustrated in Fig. 1 for the case of our two-well toy system, the resulting time line has a staircase-like structure where the system always remains in one state for the time t to $t + \Delta t_{\rm escape}$ before it hops to the next state.

Obviously, $\Delta t_{\rm escape}$ is determined by the rate constants and in order to derive the exact relationship required for the kMC algorithm let us stay with the two-well example. In this system there is always only one possibility where to go next. If in state A there is the possibility to jump into state B with a probability expressed by the rate constant k_{AB}, and if in state B there is the possibility to jump into state A with a probability prescribed by the rate constant k_{BA}. Now, one of the fundamental ideas behind the entire kMC approach is that during its thermal vibrational motion in one of the PES basins the system loses the memory of its past history. Carrying this picture one step further one may assume that this loss of memory occurs continuously, so that the system has the same probability of finding the escape path during each short increment of time it spends in the PES basin. This leads to an exponential decay statistics, i.e. the probability that the system has e.g. escaped from state A into state B after a time Δt is $1 - \exp(-k_{AB}\Delta t)$. The connected probability distribution function for the time of first escape $p_{AB}(\Delta t)$ is just the time derivative of this and is a Poisson distribution,

$$p_{AB}(\Delta t) \;=\; k_{AB}\,\exp\left(-k_{AB}\Delta t\right) \quad , \tag{2}$$

centered around the average time for escape given by $\overline{\Delta t}_{\rm escape} = k_{AB}^{-1}$. When only considering this average time for escape, an executed jump from state A to state B would therefore simply advance the system clock by $t \to t + \overline{\Delta t}_{\rm escape}$. Formally more correct is, however, to advance the system clock by an escape time that is properly weighted by the probability distribution function $p_{AB}(\Delta t)$.[16,17] Generating such an exponentially distributed escape time is numerically achieved through the expression

$$\Delta t_{\rm escape} \;=\; -\frac{\ln(\rho)}{k_{AB}} \quad , \tag{3}$$

where $\rho \in]0,1]$ is a random number. Equally, a jump from state B to A would advance the system clock by an exponentially distributed time $-\ln(\rho)/k_{BA}$. If, as in the example in Fig. 1, basin B has a lower stability, then the probability to jump out of this shallower well will obviously be larger than jumping out of the deeper well A, i.e. $k_{BA} > k_{AB}$. After Eq. (3), this means that the typical escape time out of A will be larger than out of B as illustrated by the schematic timeline also shown in Fig. 1. Averaged over a sufficiently long time, we therefore arrive at the expected result that the system spends more time in the more stable state.

Generalizing the escape time procedure to realistic systems with a manifold of different states i is straightforward.[17] Because of its loss of memory, the system has at any moment in time a fixed probability to find any one of the now many possible pathways out of the present minimum, with the fixed probabilities for the

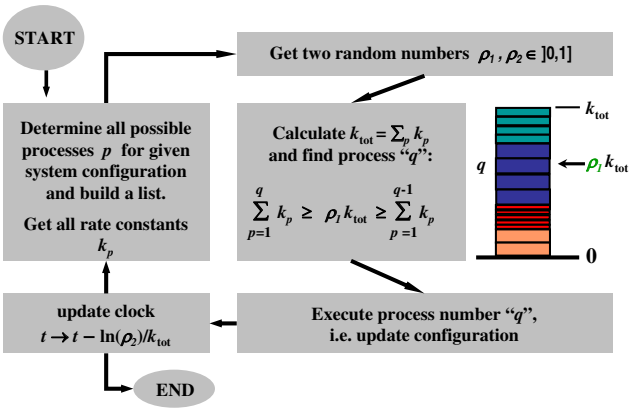

FIG. 3: Flow chart illustrating the basic steps in the rejection-free BKL algorithm. The loop starts with the determination of all processes (and their rate constants) that are possible for the current system configuration. After the generation of two random numbers, the system is advanced according to the process selected by the first random number and the system clock increments according to the computed total rate constant and the second random number, as prescribed by an ensemble of Poisson processes. Thereafter the loop starts anew, or the simulation is terminated, if a sufficiently long time span has been covered.

different pathways given by the different rate constants. Each pathway has thus its own probability distribution function for the time of first escape. Say, if we are currently in state i, we have for each possible pathway to another state j a Poisson distribution

$$p_{ij}(\Delta t) \;=\; k_{ij}\,\exp\left(-k_{ij}\Delta t\right) \quad . \tag{4}$$

Since only one event can be the first to happen, an intuitive generalization to propagate the kMC trajectory, also known as the first-reaction method[18], would be to draw a random number for each possible pathway and therewith determine for each one of them an exponentially distributed escape time through an expression of the form of Eq. (3). We then pick the pathway with the shortest escape time, move the system to the state reached by that pathway, advance the system clock by the corresponding shortest escape time, and begin again from the new state. Even though this is a perfectly valid kMC algorithm, it is clearly not particularly efficient, as we have to draw a lot of random numbers to generate all the different escape times and then discard all but one of them.

Among a variety of numerically efficient kMC algorithms suggested in the literature[19,20], the one most commonly used in practice is often attributed to Bortz, Kalos and Lebowitz[21] even though one can clearly trace its idea back further[8]. As such, it is sometimes referred to as the BKL algorithm, with the "N-fold way", residence-time algorithm or Gillespie algorithm being other frequently employed names. Figure 3 compiles a flowchart of this algorithm. As necessarily required in any kMC procedure, it starts with the determination of all N possible processes, aka escape pathways, out of the present system configuration, aka state. The corresponding N different rate constants are then summed to yield the total rate constant

$$k_{\rm tot} \;=\; \sum_{p=1}^{N} k_p \quad . \tag{5}$$

Executed is the process q, which fulfills the condition

$$\sum_{p=1}^{q} k_p \;\geq\; \rho_1 k_{\rm tot} \;\geq\; \sum_{p=1}^{q-1} k_p \quad , \tag{6}$$

where $\rho_1 \in]0,1]$ is a random number. In order to understand the idea behind this condition imagine for each process p a block of height k_p. If we then stack all of these blocks on top of each other as illustrated in Fig. 3, we arrive at a stack of total height $k_{\rm tot}$. Choosing a random height along this stack, i.e. $0 < \rho_1 k_{\rm tot} \leq k_{\rm tot}$, will point to one of the blocks and this is the process that is selected. Obviously, a process with a large rate constant, i.e. a large block height, has a higher chance of being chosen in this way, and this probability weighted selection is precisely what the partial sums in Eq. (6) achieve. By executing the selected process the system is moved to the new configuration, the system clock is advanced by

$$t \;\rightarrow\; t - \frac{\ln(\rho_2)}{k_{\rm tot}} \quad , \tag{7}$$

where $\rho_2 \in]0,1]$ is another random number, and the entire cycle starts anew from the new system state. Instead of drawing N different random numbers for the N possible pathways as in the intuitive first-reaction method, this algorithm thus needs only two in each cycle, which in case of realistic systems of the type discussed below makes a huge computational difference. Each cycle furthermore definitely propagates the system to a new state, which is also often viewed as an advantage of the corresponding class of "rejection-free" kMC algorithms.

An important aspect of the BKL algorithm is that the time by which the clock is advanced, cf. Eq. (7), is independent of which process was actually chosen. To understand this it is important to realize that the overall scale of $\Delta t_{\rm escape}$ is governed by the fastest process that can occur in a given configuration. This process with the highest rate constant has the shortest average escape time, cf. Eq. (4), and even in the maybe more intuitive first-reaction method a slower process has only a chance of getting selected if its randomly drawn escape time is of this order of magnitude. Since the Poisson distribution of this slower process is centered around a longer average escape time, this happens only rarely and correspondingly the slow process occurs less often than the fast ones in the generated kMC trajectory as should be the case. In

the BKL algorithm this differentiation between slow and fast processes is instead achieved through the probability weighted selection of Eq. (6). Nevertheless, since the overall magnitude of $k_{\rm tot}$ is predominantly determined by the high rate constant processes, the amount of time by which the clock is advanced after the execution of a process, cf. Eq. (7), is equally reduced as soon as a fast process is possible. The same argument holds of course for increasing system sizes. Larger system size typically means more processes that can occur. With more terms in the sum in Eq. (5) $k_{\rm tot}$ gets larger, similarly reducing the time increment achieved by the individual kMC steps and thereby limiting the total simulation times that can be reached.

In this respect, we see that the often made statement that kMC enables simulation time up to seconds or longer is a bit sloppy. The total simulation time that can be reached depends instead on the system size and predominantly on the fastest process in the system, both of which dictate the increment in time typically achieved by one kMC step. If the system features a process that happens on a nanosecond time scale, it is this process and not the possibly more relevant less frequent ones that will virtually always be executed. Each kMC step then advances the time also only on the order of a nanosecond, which may therewith well become a bottleneck for the simulation. When people hence refer to the macroscopic times that can be reached with kMC simulations, this simply means that the fastest processes in the particular problems and system sizes they studied allowed them to do so – or that they resorted to some of the known tricks to address this problem (*vide infra*). In fact, it depends on the physics of the problem what simulation times are required, and even when "only" achieving say microseconds, a kMC simulation may still be an enormous asset. This said, the limitations set by the presence of very fast processes are one of the current frontiers of this method to which I will return at the end of this Chapter.

D. Transition-state theory

From the preceding discussion it is clear that the efficiency of a kMC simulation in tackling the long-time evolution of rare-event systems arises from the fact that the short-time vibrational motion around the individual PES basins is appropriately coarse-grained into the rate constants k_{ij}. Up to now we have, however, simply assumed that these probabilities for the hops between the different system states are known. Obviously, if one only aspires a conceptual discussion, one could use here *ad hoc* values that either fall purely from heaven or are (with more or less justification) believed to be somehow "characteristic" for the problem. In fact, the original development of kMC theory was done within this kind of approach[9,16–18,21,22] and by now there is an entire bulk of literature where kMC simulations have been used in this sense. As stated in the introduction, the idea (and value) of modern first-principles kMC simulations is instead to be material-specific, and in the philosophy of hierarchical models, to carry the predictive power of first-principles electronic structure theories to the mesoscopic scale.[2] For this type of modeling based on a proper microscopic meaning, an important aspect is then to derive a stringent relationship between the rate constants k_{ij} and the PES information provided from the first-principles theories.

As a first step in this derivation let us consider the constraints coming from the master equation for a system that has reached steady state. With a vanishing time derivative in Eq. (1), we arrive at one condition

$$\sum_{j\neq i} \left[k_{ij} P_i^* \; - \; k_{ji} P_j^* \right] \; = \; 0 \qquad (8)$$

for every state i, where P_i^* and P_j^* are the time-independent probabilities that the steady-state system is in state i and j, respectively. This condition states that at steady state the sum of all transitions into any particular state i equals the sum of all transitions out of this state i. Since such a condition holds for every single state i in the system, the manifold of such conditions is in general only fulfilled, if every term in the sum in Eq. (8) separately equals to zero,

$$\frac{k_{ij}}{k_{ji}} \; = \; \frac{P_j^*}{P_i^*} \quad . \qquad (9)$$

This is the detailed balance (or microscopic reversibility) criterion[6], which holds independently for the transitions between every pair of states i and j in the system. If the system has furthermore reached thermodynamic equilibrium with respect to the population of these two states, then the fractional population of states i and j on the right hand side of Eq. (9) is simply proportional to the Boltzmann weighted difference in the free energies of these two states. For say the case of our surface diffusion model and the two bound states of different stability, A and B, we would have the condition

$$\frac{k_{AB}}{k_{BA}} \; = \; \exp\left(-\frac{F_B(T) - F_A(T)}{k_B T} \right) \quad , \qquad (10)$$

where k_B is the Boltzmann constant, and $F_A(T)$ and $F_B(T)$ are the free energies of states A and B, respectively, comprising each the total energy of the state and its vibrational free energy at the temperature T.

The detailed balance relation places some constraints on the rate constants, and the PES information entering are the relative energies of the different states and their vibrational properties, i.e. data about the (meta)stable minima. For just the evaluation of equilibrium properties, no further specification of the rate constants is in fact needed. Based on knowledge of the PES minima equilibrium Monte Carlo (MC) algorithms like the one due to Metropolis[23] or due to Kawasaki[24] thus construct

their transition probabilities according to detailed balance. In this respect, it is worth noting that in a dynamical interpretation, the resulting MC trajectories can therefore also be seen as numerical solutions to the master equation, Eq. (1). This holds only for the equilibrated system though. While it is admittedly tempting to also assign some temporal meaning e.g. to the initial part of a MC trajectory when the system has not yet reached equilibrium, it is important to realize that a MC step does in general not correspond to a fixed amount of real time.[15] Only kMC algorithms propagate the system properly in time, and for this they need the absolute values of the rate constants, not just the relative specification as achieved by detailed balance.[17] The latter criterion is nevertheless an important constraint, in particular in light of the frequently quite approximate determination of the rate constants to be discussed below. If (inadvertently) different and inconsistent approximations are made for the forward and backward rate constants between any two states, detailed balance is violated and the corresponding kMC simulations will never attain the correct thermodynamic limits.

At present, the most commonly employed approach to obtain the absolute values of the rate constants in first-principles kMC simulations in the area of surface chemistry and catalysis is transition-state theory (TST)[25–27]. In TST, the rate constant for the transition from state A to state B in our two-well toy system is approximated by the equilibrium flux through a dividing surface separating the two states: Imagine creating an equilibrium ensemble by allowing a large number of replicas of this two-state system to evolve for a sufficiently long time that many transitions between the two states have occurred in each replica. If we then count the number of forward crossings through a dividing surface separating state A and B that occur per unit time in this ensemble, and divide this by the number of trajectories that are on average in state A at any time, this yields the TST approximation to the rate constant, k_{AB}^{TST}. Apart from the assumed equilibrium, another important implicit assumption is here that successive crossings through the dividing surface are uncorrelated in the sense that each forward crossing takes the system indeed from state A to state B. In reality, there is, of course, the possibility that a trajectory actually recrosses the dividing surface several times before falling either into state A or state B. Since this leads to k_{AB}^{TST} overestimating the real rate constant, the best choice of dividing surface is typically near the ridge top of the PES, where recrossings and in fact the entire equilibrium flux is minimized.[27]

In this respect, it comes as no surprise that in harmonic TST (hTST)[28], the dividing surface is actually taken to be the hyperplane perpendicular to the reaction coordinate at the maximum barrier along the minimum-energy path connecting the two states, with the understanding that the equilibrium flux occurs predominantly through this one transition state. With the additional approximation that out to the displacements sampled by the thermal motion the PES around the minimum and at the saddle point (in the dimensions perpendicular to the reaction coordinate) is well described by a second-order expansion, i.e. that the corresponding vibrational modes are harmonic, this then leads to very simple expressions for the rate constants.[27] For the transition between the two bound states in Fig. 1 one can e.g. derive the form[29]

$$k_{AB}^{\mathrm{TST}}(T) \;=\; f_{AB}^{\mathrm{TST}}(T)\,\left(\frac{k_B T}{h}\right)\,\exp\left(-\frac{\Delta E_{AB}}{k_B T}\right) \quad , \tag{11}$$

where h is Planck's constant and

$$f_{AB}^{\mathrm{TST}}(T) \;=\; \frac{q_{\mathrm{TS}(AB)}^{\mathrm{vib}}}{q_A^{\mathrm{vib}}} \quad . \tag{12}$$

Here, ΔE_{AB} denotes the energy barrier between the two sites, $q_{\mathrm{TS}(AB)}^{\mathrm{vib}}$ the partition function at the transition state, and q_A^{vib} the partition function at the bound state A.

With a corresponding expression for the backward rate constant k_{BA}^{TST}, the form of Eq. (11) naturally fulfills the detailed balance condition, cf. Eq. (10). Equally important is to realize that because k_{AB}^{TST} is an equilibrium property, there is no need to ever perform any actual dynamical simulations. Instead, only static PES information is required in form of the energies at the initial state minimum and at the transition state, as well as the curvature around these two points for the harmonic modes. It is this efficiency of hTST that largely explains its popularity in first-principles kMC simulations, where as we will further discuss below every single energy and force evaluation "hurts". The other reason is that hTST tends to be a quite good approximation to the exact rate constant for the typical processes in surface chemical applications, like diffusion or surface reaction events with a tight transition state. Loosely speaking, the making and breaking of strong covalent bonds involved in these processes seems to give rise to rather smooth PES landscapes, with deep troughs and simply structured ridges in between. These (anticipated) characteristics do not necessarily call for more elaborate reaction rate theories like transition-path sampling[30] or even just more refined TST versions like variational TST[31], in particular as all these approaches require significantly more PES evaluations and thus come at a significantly higher computational cost in first-principles kMC.

In fact, with the vibrational properties of atomic or small molecular adsorbates at minimum and transition state often found to be rather similar, and hence $f_{AB}^{\mathrm{TST}}(T) \sim 1$, practical work has on the contrary frequently even dodged the vibrational calculations and resorted instead to the yet more crude approximation of setting the prefactor simply constant to $k_{\mathrm{B}}T/h \approx 10^{13}\,\mathrm{s}^{-1}$ for temperatures around room temperature. Especially with applications in surface chemistry and catalysis (involving larger molecules) in mind, one needs to stress in this respect that this procedure is not generally valid and does e.g. certainly not apply to unactivated

adsorption processes, where the prefactor needs to account for the strong entropy reduction in going from the gas-phase to the bound state at the surface. Assuming at a local partial pressure p_n of species n of mass m_n an impingement as prescribed by kinetic gas theory, the starting point for the calculation of the rate constant e.g. into site B is then the expression[29],

$$k_{n,B}^{\rm ads}(T,p_n) \;=\; \tilde{S}_{n,B}(T)\,\frac{p_n A_{uc}}{\sqrt{2\pi m_n k_B T}} \quad , \qquad (13)$$

where the local sticking coefficient $\tilde{S}_{n,B}(T)$ governs which fraction of these impinging particles actually sticks to a free site B, and A_{uc} is the area of the surface unit-cell containing site B. The determination of the local sticking coefficient dictates in principle explicit dynamical simulations, which in practice may again be avoided by resorting to some approximate treatments. Defering the reader to ref. [29] for a detailed discussion of this point, suffice it here to repeat that in this case or when in general resorting to approximations in the rate constant determination particular care has to be exerted that this does not infer a violation of detailed balance.

E. First-principles rate constants and the lattice approximation

Within the hTST framework, the most important PES information entering the determination of a rate constant is apart from the (meta)stable minimum the location of the transition state. In the surface catalytic applications on which we focus here, the latter region of the PES corresponds typically to the situation where chemical bonds are made or broken. This fact imposes an important constraint, when now considering which methodology to use that would provide the required PES data. Electronic-structure theories[3,4], comprising *ab initio* quantum chemistry as well as density-functional methods, explicitly treat the electronic degrees of freedom and are therefore the natural base for such a modeling. However, in view of the high computational cost incurred by these techniques, and considering that for the rate constant determination only the ground-state energy and not the additionally provided detailed electronic structure data is necessary, an appealing approach would be to condense the information into a suitably parameterized interatomic potential. Such potentials (or force fields) then yield the energy and forces solely as a function of the nuclear positions and do so at a significantly reduced computational cost. While this approach appears to be highly successful e.g. in the area of biophysical applications and finds widespread use in applied materials research, it is crucial to realize that few, if any of the existing atomistic potentials can deal with the complex charge transfer or changes in hybridization that are critical when bond breaking or bond making plays a role. When really aspiring a material-specific and predictive-quality modeling of surface chemistry, the quantum mechanical nature of the chemical bonds needs therefore to be explicitly treated, dictating the use of electronic-structure theories to generate what is then commonly called first-principles rate constants.

For the extended metal or compound surfaces encountered in catalytic problems, DFT is currently the main workhorse among the electronic-structure theories. Deferring to excellent textbooks for details[32–34], the decisive gist of this technique is that all complicated many-body effects of the interacting electron gas are condensed into the so-called exchange and correlation functional. The exact form of this functional remains elusive, necessitating the use of approximate functionals[35], with local (local-density approximation, LDA) and semi-local (generalized gradient approximation, GGA) functionals still forming the most widely employed class in current applications[5]. While exact in principle, DFT in practice is thus not, and, moreover, does mostly not even meet the frequent demand for "chemical accuracy" (1 kcal/mol $\approx$ 0.04 eV) in the energetics.[36] As studies of the kind illustrated in the next Section only become computationally feasible at all by the unbeaten efficiency of DFT, this uncertainty is something that must be kept in mind at all times and we will return to a more detailed analysis of its consequences towards the end of this Chapter. With expected typical errors in DFT-LDA or DFT-GGA barriers of the order of say ~ 0.2 eV, this also further justifies the use of a crude reaction rate theory like hTST in most existing first-principles kMC work: With such an error entering the exponential in the rate constant expression, Eq. (11), worrying about a more elaborate determination e.g. of the prefactor may not be the most urgent issue. Just to set these critical remarks into perspective though, let me stress that DFT is at present the method of choice. With not many (semi-)empirical potentials on the market that are parameterized to deal with molecules at metal or oxide surfaces anyway, qualitatively wrong barriers with errors exceeding ~ 1 eV (and therewith often completely wrong hierarchies in the process rate constants) would not be uncommon for any of them. If one thinks kMC based on DFT rate constants has problems, then simulations based on barriers from semi-empirical potentials are completely pointless.

Getting DFT energies and forces for reactions at extended metal or compound surfaces is typically achieved using so-called supercell geometries.[37,38] With the technicalities of such calculations e.g. reviewed by Payne *et al.*[39], suffice it here to say that this automatically implies having to deal with rather large systems. In view of the huge computational cost connected to such calculations one will consequently want to make sure that obtaining the required PES information and, in particular, locating the transition state, can be done with as little energy and force evaluations as possible. In mathematical terms, locating the transition state means identifying a saddle point along a reaction path on a high-dimensional surface. Completely independent of the computational constraints, this is not at all a trivial problem, and the development of efficient and reliable transition-state search al-

gorithms is still a very active field of current research.[40,41] Among a variety of existing approaches, string algorithms like climbing-image nudged elastic band[42,43] enjoy quite some popularity in surface reaction studies, and are by now included in most of the modern DFT software packages. Despite this ready availability, caution is always advised with these algorithms as none of them is fool-proof. In particular if existing symmetries can be efficiently exploited to reduce the dimensionality of the problem, mapping the PES along a couple of suitable reaction coordinates might therefore always be a worthwhile alternative, that in addition provides also more insight into the overall topology of the PES than just knowing where the saddle point is.

In either approach, identification of the transition state and the ensuing calculation of the rate constant for an individual pathway using DFT energies and forces is nowadays typically computationally involved, but feasible. However, the more different processes there are, the more calculations are necessary. The feasibility statement holds therefore only if the total number of independent rate constant calculations, i.e. primarily the expensive transition-state searches, remains finite, if not small. In order to ensure this, first-principles kMC simulations resort up to now almost exclusively to a lattice mapping in conjunction with the thereby enabled exploitation of locality. Let me explain this concept again on the basis of the surface diffusion problem. Quite characteristic for many problems in surface catalysis the adsorbate considered in this example shows a site-specific adsorption. In the case of a simple single-crystal surface it is then straightforward to map the total diffusion problem onto the periodic lattice formed by these sites, say a cubic lattice in the case of adsorption into the hollow sites of a fcc(100) surface. On this lattice a single diffusion event translates simply into a hop from one discrete site to another one, and the advantage is that one has a unique specification of a given system state i just on the basis of the population on the different lattice sites. If one now constructs a catalog of possible processes and their corresponding rate constants for every possible state on the lattice before the kMC simulation, one can check at every kMC step the configuration on the lattice, identify the state and then perform the random selection which process is executed at essentially zero computational cost by looking up the processes and their rate constants in the catalog.[44]

The lattice mapping together with the rate constant catalog achieves already that the total number of rate constants that needs to be computed is finite. A significant reduction of this number that ultimately makes the simulations feasible is thereafter achieved by considering the locality of most surface chemical processes. Assume in the simplest case that the diffusion process of the adsorbate would not be affected at all by the presence of other nearby adsorbates, apart from the fact that no diffusion could occur into any already occupied sites. Despite an astronomically large number of different system states corresponding each to a different spatial distribution of a given number of adsorbates on the lattice, only one single rate constant would need to be computed, namely the rate constant for the pathway of a hop from one site to the next. Admittedly, such a situation with a complete absence of lateral interactions between the adsorbates is rarely realized. Nevertheless, nothing prevents us from extending the dependence on the local environment. Staying with the diffusion problem, imagine that the diffusion process is now only affected by the presence of other adsorbates in nearest neighbor sites. For the illustrative example of just one adsorbate species on a cubic lattice this means that – regardless of the occupation of more distant lattice sites – now five different rate constants need to be computed as illustrated in Fig. 4: One for the diffusion process of an "isolated" adsorbate without any nearest neighbors, two with one nearest-neighbor site occupied, as well as one with two and one with three such sites occupied (if all four nearest-neighbor sites are occupied, the adsorbate obviously cannot move via a nearest-neighbor hop, so no rate constant calculation is required here). If the diffusion process depends furthermore on how the neighbors are arranged around the diffusing adsorbate, further rate constants could be required, e.g. to distinguish the situation with two neighbors either located on diagonal neighboring sites of the adsorbate as in Fig. 4 or not. Consideration of an increasing local environment thus increases the number of

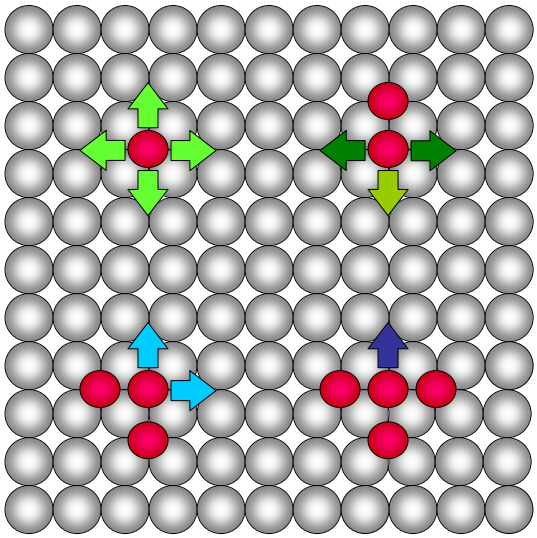

FIG. 4: Schematic top view illustrating the effect of lateral interactions with the nearest-neighbors in the surface diffusion problem with one atomic surface species and site-specific adsorption into the hollow sites of a fcc(100) lattice. Consideration of such lateral interactions requires the computation of five different rate constants, corresponding to the motions sketched with differently colored arrows, see text (small red spheres = adsorbate, large gray sphere = substrate atoms).

inequivalent rate constants that need to be computed, and this number increases steeply when accounting for the constellation in the second, third and so on nearest-neighbor shells. On the other hand, depending on the nature of the surface chemical bond such lateral interactions also decay away more or less quickly with distance, so that either a truncation or a suitable interpolation[45] is possible, in either case with only a quite finite amount of different DFT rate constant calculations remaining.

This leaves the problem of how to determine in the first place which lateral interactions are actually operative in a given system, keeping additionally in mind that lateral interactions especially at metal surfaces are by no means necessarily restricted to just the pairwise interactions discussed in the example. For site-specific adsorption the rigorous approach to this problem is to expand DFT energetics computed for a number of different ordered superstructures into a lattice-gas Hamiltonian.[2]. This cluster expansion technique[46–48] is to date primarily developed with the focus on lateral interactions between surface species in their (meta)stable minima[2,45,49–53], but generalizing the methodology to an expansion of the local environment dependence of the transition states is straightforward. Due to the computational constraints imposed by the expensive transition-state searches, existing expansions in first-principles kMC work in the field are often rather crude, truncating the dependence on the local environment often already at the most immediate neighbor shells. In this situation, it has been suggested[54] that a less rigorous alternative could be to resort to semi-empirical schemes like the unity bond index-quadratic exponential potential (UBI-QEP) method[55] to account for the effects of the local environment. In either case, great care has again to be taken that applying any such approximations does not lead to sets of rate constants that violate the detailed balance criterion. Particularly in models with different site types and different surface species, this is anything but a trivial task.

III. A SHOWCASE

Complementing the preceding general introduction to the underlying concepts, let me continue in this Section with a demonstration of how first-principles kMC simulations are put into practice. Rather than emphasizing the breadth of the approach with a multitude of different applications, this discussion will be carried out using one particular example, namely the CO oxidation at $RuO_2(110)$. With a lot of theoretical work done on the system, this focus enables a coherent discussion of the various facets, which I feel is better suited to provide an impression of the quality and type of insights that first-principles kMC simulations can contribute to the field of heterogeneous catalysis (with refs. 56,57 e.g. providing similar compilations for epitaxial growth related problems). Since the purpose of the example is primarily to highlight the achievements and limitations of the methodological approach, suffice it to say that the motivation for studying this particular system comes largely from the extensively discussed pressure gap phenomenon exhibited by "Ru"-catalysts, with the $RuO_2(110)$ surface possibly representing a model for the active state of the catalyst under technologically relevant O-rich feeds (see e.g. ref. [58] for more details and references to the original literature).

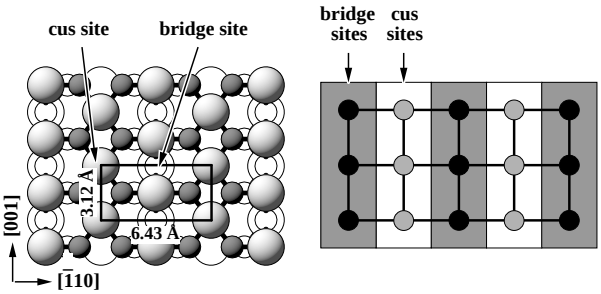

FIG. 5: Top view of the $RuO_2(110)$ surface showing the two prominent active sites (bridge and cus). Ru = light, large spheres, O = dark small spheres. When focusing on these two site types, the surface can be coarse-grained to the lattice model on the right, composed of alternating rows of bridge and cus sites. Atoms lying in deeper layers have been whitened in the top view for clarity.

A. Setting up the model: Lattice, energetics and rate constant catalog

To some extent the system lends itself to a modeling with first-principles kMC simulations, as extensive surface science experimental[59] and DFT-based theoretical studies[29] have firmly established that the surface kinetics is predominantly taking place at two prominent active sites offered by the rutile-structured $RuO_2(110)$ surface, namely the so-called coordinately unsaturated (cus) and the bridge (br) site. As illustrated in Fig. 5 this leads naturally to a lattice model where these two sites are arranged in alternating rows, and to consider as elementary processes the adsorption and desorption of O and CO at the bridge and cus sites, as well as diffusion and surface chemical reactions of both reaction intermediates adsorbed at these sites. With a very small DFT-computed CO_2 binding energy to the surface[29], the surface reactions can furthermore be modeled as associative desorptions, i.e. there is no need to consider processes involving adsorbed CO_2.

Another benign feature of this system is its extreme locality in the sense that DFT-computed lateral interactions at the surface are so small that they can be neglected to a first approximation.[29] Considering the exhaustive list of non-correlated, element-specific processes that can occur on the two-site-type lattice then leads to 26 different elementary steps, comprising the dissociative

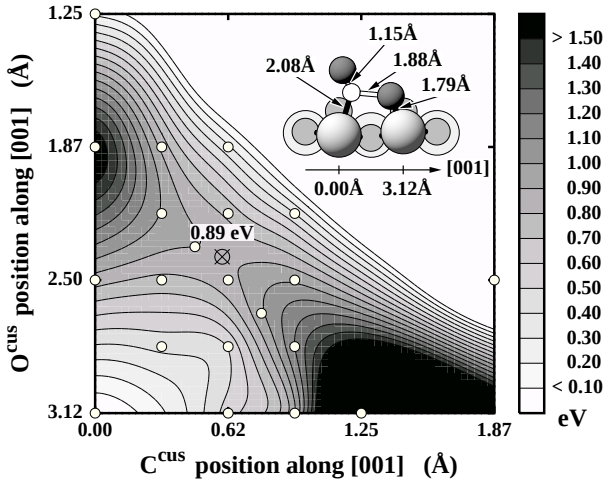

FIG. 6: Calculated DFT-PES of one of the possible CO oxidation reaction mechanisms at the $RuO_2(110)$ model catalyst surface. The high-dimensional PES is projected onto two reaction coordinates, representing two lateral coordinates of the adsorbed O^{cus} and CO^{cus} (cf. Figure 5). The energy zero corresponds to the initial state at (0.00 Å, 3.12 Å), and the transition state is at the saddle point of the PES, yielding a barrier of 0.89 eV. Details of the corresponding transition state geometry are shown in the inset. Ru = light, large spheres, O = dark, medium spheres, and C = small, white spheres (only the atoms lying in the reaction plane itself are drawn as threedimensional spheres). (From ref. [60]).

TABLE I: Binding energies, E_b, for CO and O (with respect to $(1/2)O_2$) at bridge and cus sites, cf. Fig. 5, and diffusion energy barriers, $\Delta E^{\rm diff}$, to neighboring bridge and cus sites, as used in the kMC simulations. The desorption barriers are given for unimolecular and for associative desorption with either O^{cus} or O^{br}. This includes therefore surface reactions forming CO_2, which are considered as associative desorption of an adsorbed O and CO pair. All values are in eV. (From ref. [29]).

	E_b	$\Delta E^{\rm des}$			$\Delta E^{\rm diff}$	
		unimol.	with O^{br}	with O^{cus}	to br	to cus
CO^{br}	-1.6	1.6	1.5	0.8	0.6	1.6
CO^{cus}	-1.3	1.3	1.2	0.9	1.3	1.7
O^{br}	-2.3	–	4.6	3.3	0.7	2.3
O^{cus}	-1.0	–	3.3	2.0	1.0	1.6

adsorption of O_2 resulting in three possible postadsorption states (two O atoms in neighboring cus sites, two O atoms in neighboring br sites, or two O atoms, one in a br site and one in a neighboring cus site); the associative desorption of O_2 from each of the three configurations of the O atoms; the adsorption of CO in cus or br sites; the desorption of CO from cus or br sites; the reaction of CO with O from four different initial states with the intermediates in neighboring sites (O in cus reacting with CO in cus, O in cus with CO in br, O in br with CO in br, and O in br with CO in cus); the corresponding four backreactions dissociating gas-phase CO_2 into adsorbed CO and O; and the hops of O and CO from a site to the nearest site (for all possible site combinations).

The rate constants for all these processes were calculated using DFT-GGA to determine the energy barriers and TST expressions like those of Eqs. (11) and (13), ensuring that all forward and backward processes obey detailed balance.[29] Fig. 6 shows one of the correspondingly computed PES mappings along high-symmetry reaction coordinates and Table I lists all the resulting energy barriers as used in the kMC simulations. Just to set the perspective, it is worth mentioning that it took of the order of half a million CPU-hours at the time on Compaq ES45 servers to assemble this totality of energetic information required for the rate constant catalog.

The relevant physics that emerges at the level of this energetics is that there is a strong asymmetry in the O binding to the two active sites, quite strong to the bridge sites ($\sim$ 2.3 eV/atom) and only moderate at the cus sites ($\sim$ 1.0 eV/atom). CO adsorption, on the other hand, has a rather similar strength of the order of $\sim$ 1.5 eV/atom at both sites. From the established importance of the oxygen-metal bond breaking step in catalytic cycles and the Sabatier principle[10–12] one would thus expect the O^{cus} species to be mostly responsible for the high catalytic activity of this model catalyst at high pressures. In fact, this notion, as expressed by the well-known Brønsted-Evans-Polanyi type relationships[61], is fully confirmed by the computed reaction barriers, with the two reactions involving the strongly bound O^{br} species exhibiting rather high barriers ($O^{br} + CO^{br} :\sim 1.5$ eV, $O^{br} + CO^{cus} :\sim 1.2$ eV) and the two reactions involving the moderately bound O^{cus} species exhibiting lower barriers ($O^{cus} + CO^{br} :\sim 0.8$ eV, $O^{cus} + CO^{cus} :\sim 0.9$ eV). From a mere inspection of these energetics, particularly the lowest-barrier $O^{cus} + CO^{br} \rightarrow CO_2$ reaction appears thus most relevant for the catalysis, and one would imagine it to dominate the overall activity.

B. Steady-state surface structure and composition

With the rate constant catalog established, a first important application area for kMC simulations is to determine the detailed composition of the catalyst surface under steady-state operation, i.e. the spatial distribution and concentration of the reaction intermediates at the active sites. In the absence of mass transfer limitations in the reactor setup, the reactant partial pressures entering the surface impingement, Eq. (13), can be taken as equal to those at the inlet, without build-up of a significant product concentration in the gas-phase above the working surface. If one furthermore assumes that any heat of reaction is quickly dissipated away, an approximation to steady-state operation can simply be achieved by performing the kMC simulations at constant reactant

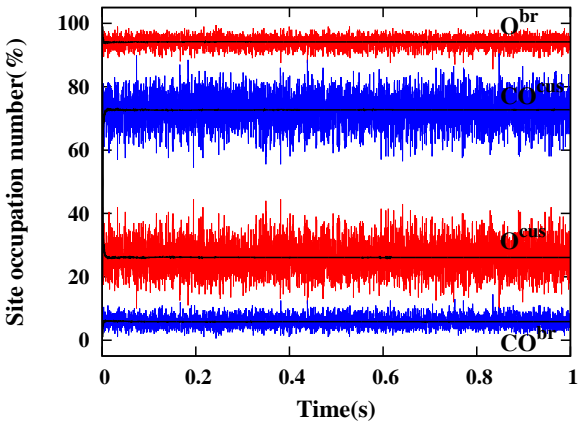

FIG. 7: Time evolution of the site occupation by O and CO of the two prominent adsorption sites, bridge and cus, cf. Fig. 5. The temperature and pressure conditions chosen ($T = 600\,\mathrm{K}$, $p_{\mathrm{CO}} = 7\,\mathrm{atm}$, $p_{\mathrm{O_2}} = 1\,\mathrm{atm}$) correspond to optimum catalytic performance (*vide infra*). Under these conditions kinetics builds up a steady-state surface population in which O and CO compete for either site type at the surface, as reflected by the strong fluctuations in the site occupations within the employed (20×20) simulation cell. Note the extended time scale, also for the "induction period" until the steady-state populations are reached when starting from a purely oxygen covered surface. (From ref. [29]).

partial pressures $p_{\mathrm{O_2}}$ and p_{CO}, at constant global temperature T, and instantly removing any formed CO_2.

Figure 7 shows the time evolution of the actual and time-averaged surface coverages for a corresponding constant $(T, p_{\mathrm{O_2}}, p_{\mathrm{CO}})$-run starting from an arbitrary initial lattice population (in this case a fully O-covered surface).[29] Despite notable fluctuations in the actual populations (characteristically determined by the size of the employed simulation cell, here a (20×20) lattice with 200 br and 200 cus sites), steady-state conditions corresponding to constant average values for all surface species are reached after some initial induction period. Although the dynamics of the individual elementary processes takes place on a picosecond time scale, this induction period can – depending on the partial pressures – take of the order of a tenth of a second even at this rather elevated temperature. At lower temperatures around room temperature, this becomes even more pronounced, and due to the decelerated rate constants the corresponding times (covered by an equivalent number of kMC steps) are orders of magnitude longer. These time scales are an impressive manifestation of the rare-event nature of surface catalytic systems, considering that in the present example the evolution to the active state of the surface involves only the kinetics at two prominent adsorption sites without any complex morphological changes of the underlying substrate. It is clearly only the efficient time coarse-graining underlying kMC algorithms that makes it possible to reach such time scales, while still accounting for the full atomic-scale correlations, fluctuations, and spatial distributions at the catalyst surface.

Performing kMC runs starting from different initial lattice configurations and with different random number seeds allows to verify if the true dynamic steady-state for a given $(T, p_{\mathrm{O_2}}, p_{\mathrm{CO}})$ environment is reached, and in the present system no indication for multiple steady-states was found[29]. In this case, the surface populations under given gas-phase conditions as obtained from averaging over sufficiently long time spans are then already well defined in the sense that no further averaging over different kMC trajectories is required. Corresponding information about the concentration of the reaction intermediates at the active sites is therefore readily evaluated for a wide range of reactive environments ranging from ultra-high vacuum to technologically relevant conditions with pressures of the order of atmospheres and elevated temperatures. One way of summarizing the obtained results is displayed in the middle panel of Fig. 8, which compiles the dominant surface species, also called most abundant reaction intermediates (MARI), at constant temperature and as a function of the reactant partial pressures.[29] Note that the total computational time to obtain such a "kinetic phase diagram"[63] is typically insignificant compared to the afore mentioned cost of assembling the first-principles rate constant catalog. In the present system this is particularly pronounced, as the short correlation lengths resulting from the absence of lateral interactions enable the use of rather small simulation cells and as there is no kMC bottleneck in form of the discussed problem of a low-barrier process operating on a much faster time scale than all others.

At first glance, the overall structure of Fig. 8 is not particularly surprising. In O-rich environments the surface is predominantly covered with oxygen, in CO-rich environments the surface is predominantly covered with CO, and in between there is a transition from one state to the other which coincides with O and CO both being present at the surface in appreciable amounts. Such a transition from O-poisoned to CO-poisoned state depending on the partial pressure ratio is intuitive and conceptually already grasped e.g. by the early ZGB-model[64]. The real advance brought by the first-principles kMC simulations is that this information is not only provided for a generic model, but specifically for the $RuO_2(110)$ system and without empirical input. Unlike in macroscopic engineering-type models as e.g. through the MARI approximation the dominant surface species are thus not assumed, but come out as the result of the proper evaluation of the statistical interplay of microscopically correctly described elementary processes.

This rigorous solution of the master equation, cf. Eq. (1), is also what distinguishes kMC simulations from more approximate theories that are otherwise equally built on a microscopic reaction mechanism as concerns a set of elementary processes and their rate constants. In prevalent microkinetic modeling the master equation is simplified through a mean-field approximation, leading

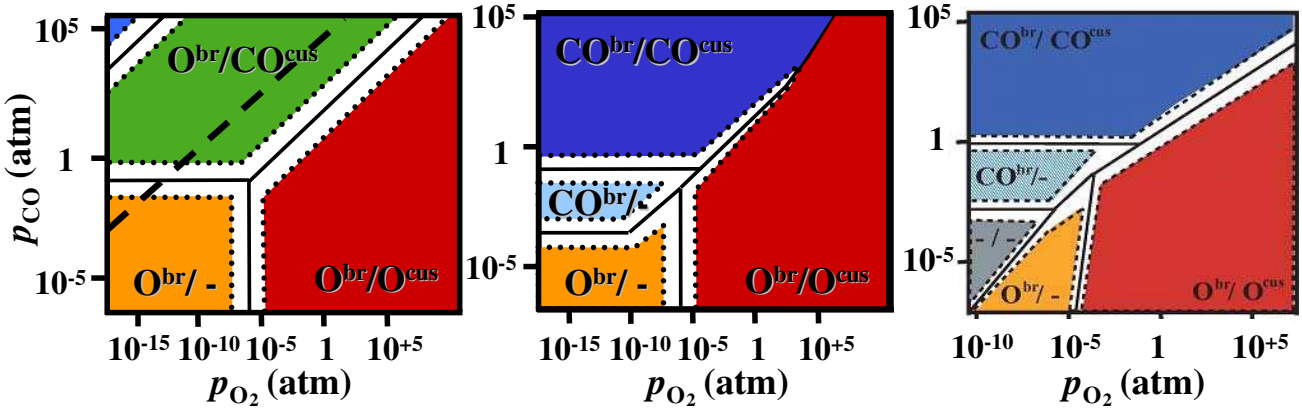

FIG. 8: Steady-state surface composition of $RuO_2(110)$ in an O_2/CO environment at $T = 600\,K$. In all non-white areas, the average site occupation is dominated ($> 90\,\%$) by one species, i.e. either O, CO or empty sites ($-$). The labels correspondingly characterize the surface populations by indicating this majority species at the bridge and cus sites. In the white regions there is a more complex coexistence of reaction intermediates and vacancies at the active sites. Compared are the results obtained by the first-principles kMC simulations (middle panel) to more approximate theories: *Constrained* atomistic thermodynamics (left panel) and microkinetic rate equations (right panel). Above the dashed line in the left panel, bulk RuO_2 is thermodynamically unstable against CO-induced decomposition, see text. (From refs. [29,60,62]).

to a set of coupled rate equations for the average concentrations of the different surface species.[11,12,65] *Constrained* atomistic thermodynamics, on the other hand, neglects the effect of the on-going catalytic reactions and evaluates the surface populations in equilibrium with the reactive environment.[60,66] Essentially it thus corresponds to a kMC simulation where the reaction events are switched off, but because of its equilibrium assumption gets away with significantly less first-principles calculations. To better assess how these approximations can harm the theory, it is instructive to compare the results obtained with the three techniques when using always exactly the same input in form of the described set of elementary processes and DFT rate constants for the CO oxidation at $RuO_2(110)$. The corresponding "kinetic phase diagrams" are shown in Fig. 8, from where one can directly see that in terms of the overall topology the rate equation approach comes rather close to the correct kMC solution.[62] Quantitatively, there are, however, notable differences and we will return to this point in more detail below. In the case of *constrained* atomistic thermodynamics the deviations under some environmental conditions are much more substantial, yet to be expected and easily rationalized.[60,66] They concern prominently the presence of the strongly-bound O^{br} species. For the thermodynamic approach only the ratio of adsorption to desorption matters, and due to its very low desorption rate, O^{br} is correspondingly stabilized at the surface even in highly CO-rich feeds. The surface reactions, on the other hand, are a very efficient means of removing this O^{br} species, and under most CO-rich conditions they consume the surface oxygen faster than it can be replenished from the gas-phase. Theories like kMC and the rate equation approach that explicitly account for the surface reactions then yield a much lower average surface concentration of O^{br} than the thermodynamic treatment, and as a consequence show an extended stability range of surface structures with CO^{br} at the surface (i.e. the $CO^{br}/-$ and CO^{br}/CO^{cus} regions in Fig. 8).

Particularly the stability of these structures under rather CO-rich conditions has to be considered with care though. In such reducing environments one would expect a CO-induced decomposition of the entire RuO_2 substrate to Ru metal, and the dashed line in the left panel of Fig. 8 represents a thermodynamic estimate where this instability of the oxide bulk sets in.[67] Considering only the kinetics involving br and cus sites of an otherwise fixed lattice, neither kMC nor rate equations account for this instability, but yield at maximum a completely CO-covered surface. With its ability to quickly compare the stability of structures with completely different morphology, the *constrained* atomistic thermodynamics approach can in this respect be seen as a nice complement to the otherwise more accurate kinetic theories. Relevant for the ensuing discussion is also that the transition from O-poisoned to CO-poisoned surface, which as we will see below corresponds to catalytically most relevant environments, is quite far away from the oxide instability limit. Under any such conditions the kinetics determining the catalytic function concentrates on the br and cus sites, and the lattice model underlying the first-principles kMC simulations is fully justified.

With its explicit account of the reaction kinetics, it is needless to stress that kMC simulations do, of course, also yield the correct temperature dependence. This is exemplified in Fig. 9, which displays the "kinetic phase diagram" obtained at $T = 350\,K$.[29] Shown is a region of

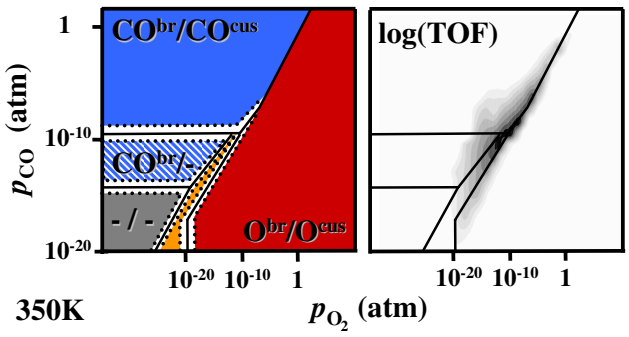

FIG. 9: Left panel: Equivalent plot of the first-principles kMC-determined surface composition as in the middle panel of Fig. 8, yet at $T = 350\,\mathrm{K}$ (see Fig. 8 for an explanation of the labeling). Right panel: Map of the corresponding turn-over frequencies (TOFs) in 10^{15} cm^{-2}s^{-1}: White areas have a TOF $< 10^3$ cm^{-2}s^{-1}, and each increasing gray level represents one order of magnitude higher activity. Thus, the black region corresponds to TOFs above 10^{11} cm^{-2}s^{-1}, while in a narrow (p_{CO}, p_{O_2}) region the TOFs actually peak over 10^{12} cm^{-2}s^{-1}. (From ref. [29]).

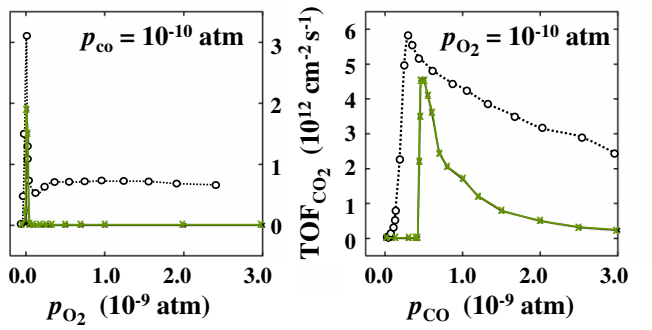

FIG. 10: Comparison of the steady-state TOFs at $T = 350\,\mathrm{K}$ from first-principles kMC (solid line) and the experimental data from Wang *et al.*[68] (dotted line). Shown is the dependence with p_{O_2} at $p_{CO} = 10^{-10}$ atm (left), and the dependence with p_{CO} at $p_{O_2} = 10^{-10}$ atm (right), cf. the overall TOF-plot in Fig. 9. (From ref. [29]).

much lower reactant partial pressures, which, however, corresponds exactly to the same range of O_2 and CO chemical potentials as in the corresponding kMC diagram at $T = 600\,\mathrm{K}$ in the middle panel of Fig. 8. This is done to briefly address the general notion of thermodynamic scaling, which expects equivalent surface conditions in thermodynamically similar gas phases and which is thus often employed to relate results from surface science studies performed under ultra-high vacuum conditions and low temperatures to catalytically relevant environments at ambient pressures and elevated temperatures. If such a scaling applies, the topology of the two diagrams at the two temperatures would be exactly the same, with only the width of the white coexistence regions varying according to the changing configurational entropy. Comparing the two kMC diagrams in Figs. 8 and 9 it is clear that scaling is indeed largely present in the sense that the transition from O-poisoned to CO-poisoned state occurs roughly at similar chemical potentials. Nevertheless, in detail notable differences due to the surface kinetics can be discerned, cautioning against a too uncritical use of thermodynamic scaling arguments and emphasizing the value of explicit kinetic theories like kMC to obtain the correct surface structure and composition at finite temperatures.

C. Parameter-free turnover frequencies

Besides the surface populations another important group of quantities that is straightforward to evaluate from kMC simulations of steady-state operation are the average frequencies with which the various elementary processes occur. Apart from providing a wealth of information illuminating the on-going chemistry, this also yields the catalytic activity as the sum of the averaged frequencies of all surface reaction events. Properly normalized to the surface area, a constant (T, p_{O_2}, p_{CO}) first-principles kMC-run thus provides a parameter-free access to the net rate of product formation or turn-over frequency, TOF (measured in molecules per area and time).

A corresponding TOF-plot for the same range of gas-phase conditions as discussed for the "kinetic phase diagram" at $T = 350\,\mathrm{K}$ is also included in Fig. 9.[29] The catalytic activity is narrowly peaked around gas-phase conditions corresponding to the transition region where both O and CO are present at the surface in appreciable amounts, with little CO_2 formed in either O-poisoned or CO-poisoned state. On a conceptual level, this is not particularly surprising and simply confirms the view of heterogeneous catalysis as a "kinetic phase transition" phenomenon[60,63,64], stressing the general importance of the enhanced dynamics and fluctuations when the system is close to an instability (here the transition from O-covered to CO-covered surface). Much more intriguing is the quantitative agreement that is achieved with existing experimental data[68] as illustrated in Fig. 10. Recalling that the calculations do not rely on any empirical input this is quite remarkable. In fact, considering the multitude of uncertainties underlying the simulations, in particular the approximate DFT-GGA energetics entering the rate constants, such an agreement deserves further comment and I will return to this point in more detail in the final frontiers Section of this Chapter.

In the catalytically most active coexistence region between O-poisoned and CO-poisoned state, the kinetics of the on-going surface chemical reactions builds up a surface population in which O and CO compete for either site type at the surface. This competition is reflected by the strong fluctuations in the site occupations visible in Fig. 7, but leads also to a complex spatial distribution of the reaction intermediates at the surface. In the absence

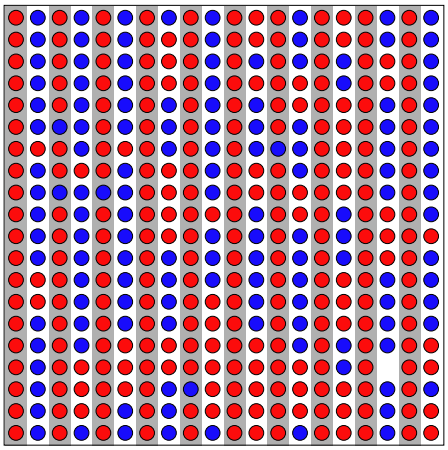

FIG. 11: Snapshot of the steady-state surface population under optimum catalytic conditions at $T = 600\,\mathrm{K}$ ($p_{O_2} = 1\,\mathrm{atm}$, $p_{CO} = 7\,\mathrm{atm}$). Shown is a schematic top view, where the substrate bridge sites are marked by gray stripes and the cus sites by white stripes, cf. Fig. 5. Oxygen adatoms are drawn as light gray (red) circles and adsorbed CO molecules as dark gray (blue) circles. (From ref. [29]).

of lateral interactions in the first-principles kMC model there is no thermodynamic driving force favoring a segregation of adsorbed O and CO. Nevertheless, as visualized by the snapshot shown in Fig. 11, a statistical analysis of the surface population reveals that they are not distributed in a random arrangement.[29] Instead they tend to cluster into small domains, which extend particularly in the direction along the bridge rows and cus trenches. This tendency arises out of the statistical interplay of all elementary processes, but emerges at the considered ambient pressures primarily from diffusion limitations and the fact that the dissociative adsorption of oxygen requires two free neighboring sites and the unimolecular adsorption of CO requires only one free site.

The resulting complex, and fluctuating spatial arrangement has important consequences for the catalytic function. As demonstrated by Fig. 12, under these conditions of highest catalytic performance it is not the reaction mechanism with the highest rate constant, i.e. the lowest-barrier reaction $O^{cus} + CO^{br} \rightarrow CO_2$, that dominates the overall activity.[29] Although the process itself exhibits very suitable properties for the catalysis, it occurs too rarely in the full concert of all possible processes to decisively affect the overall functionality. Even under most active conditions, at $T = 600\,\mathrm{K}$ e.g. for $p_{O_2} = 1\,\mathrm{atm}$ and $p_{CO} = 7\,\mathrm{atm}$, it only contributes around 10 % to the total TOF, while essentially all of the remaining activity is due to the $O^{cus} + CO^{cus} \rightarrow CO_2$ reaction mechanism.[29] This finding could not have been obtained on the basis of the first-principles energetics and rate constants alone, and emphasizes the importance of the statistical interplay and the novel level of understanding that is provided by first-principles kMC simulations. How critical it is that this evaluation of the interplay is done rigorously, is again nicely illustrated by comparing to microkinetic modeling using mean-field rate equations. As shown in Fig. 12, although using exactly the same set of elementary processes and first-principles rate constants, this theory incorrectly predicts an almost equal contribution of the two competing low-barrier reaction mechanisms to the total TOF at peak performance.[62] This peak performance (at the corresponding transition from O-poisoned to CO-poisoned surface) is furthermore obtained at slightly shifted pressure conditions as was also apparent from the "kinetic phase diagrams" in Fig. 8. The neglect of the spatial inhomogeneity in the mean-field approach thus leads to severe shortcomings, underscoring the virtue of first-principles kMC simulations to explicitly resolve the locations of all reaction intermediates at the surface.

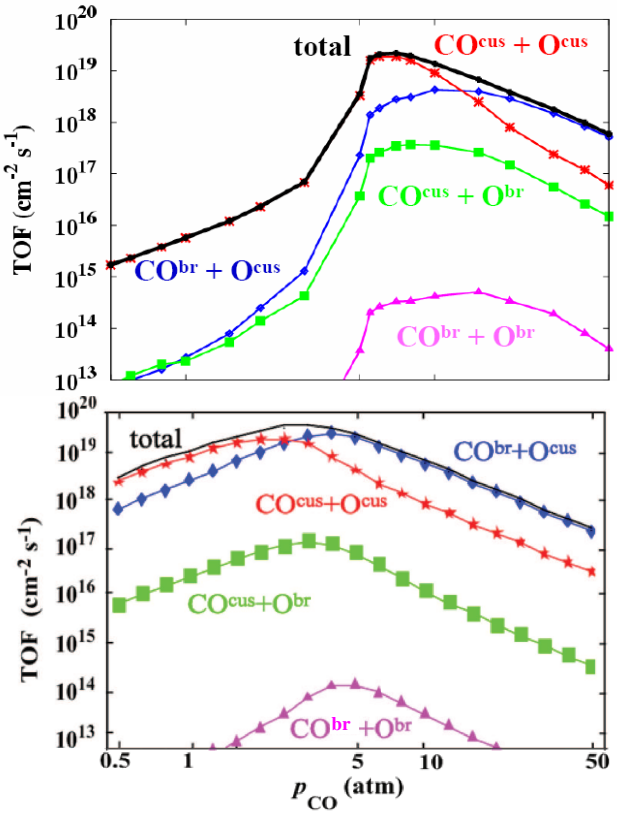

FIG. 12: Variation of the catalytic activity with CO partial pressure at $T = 600\,\mathrm{K}$ and $p_{O_2} = 1\,\mathrm{atm}$. The displayed gas-phase conditions comprise the most active state and the transition from O-poisoned to CO-poisoned surface (sketched as white region in Fig. 8). Shown is the total TOF, as well as the contribution of the four different reaction mechanisms. Upper panel: First-principles kMC. Lower panel: Microkinetic rate equations. (From ref. [62]).

In this respect, it is intriguing to notice that the microkinetic modeling yields a TOF that is about three orders of magnitude in error particularly under conditions where one would intuitively expect the mean-field approximation to be well fulfilled: The O-poisoned state

at the lowest pressures shown in Fig. 12 on the left. The reason for this deficiency even at an almost perfectly homogeneous surface coverage is that mean-field assumes the random existence of independent vacant sites with the probability of neighboring divacancies (created by associative desorption of O_2 molecules or required for dissociative adsorption of gas-phase O_2) correspondingly being proportional to the vacancy concentration squared, $\theta^2_{\rm vac}$. However, due to severe diffusion limitations particularly along the cus site trenches, divacancies created through oxygen desorption persist for such a long time that they completely dominate the total vacancy concentration at the surface. Rather than going as $\theta^2_{\rm vac}$, the probability for a divacancy is thus close to half the probability of a single vacancy, $\approx \theta_{\rm vac}/2$. If one patches the oxygen adsorption expression in the rate equations accordingly, a TOF virtually identical to the kMC result is obtained.[69]

This trick works, of course, only for gas-phase conditions corresponding to the O-poisoned surface, and incorrect TOFs are then obtained e.g. in the CO-poisoned state. This nothing but exemplifies the well-known difficulties of effectively correcting a rate equation formulation to at least partly account for site correlations. KMC on the other hand, does not suffer from this deficiency, and fully includes all correlations and stochastic fluctuations at the active surface sites into the modeling. In this context it is important to realize that another way of patching up deficiencies in the statistical modeling is to resort to effective kinetic parameters. If one considers all rate constants in the mean-field rate equation model not to be fixed by the underlying first-principles calculations, but instead to be free parameters, it is possible to achieve a perfect fit to the kMC TOF-profile shown in Fig. 12.[62,69] However, the result is just an effective description, with the optimized rate constants no longer having any kind of microscopic meaning and deviating in their values from the true first-principles rate constants underlying the kMC TOF-profile by several orders of magnitude. Not surprisingly, this effective description works only inside the parameterized range, and is not transferable to gas-phase conditions outside those shown in Fig. 12, where it predicts grossly wrong catalytic activities.

This highlights a crucial conceptual point: A hierarchical technique like first-principles kinetic Monte Carlo that builds on microscopically well-defined parameters is not only substantially more involved than existing empirical approaches because of the intense first-principles calculations, but also because it typically requires a significantly improved description at all ensuing levels, here the solution of the statistical-mechanics problem. Effective parameters, as e.g. rate constants fitted to experimental data, provide the possibility to (at least partly) cover up deficiencies in the modeling. In the present context this either means that one can get away with mean-field rate equations despite existing site correlations or that one can get away with a significantly reduced number of kMC processes that then represent some unspecified lump sum of not further resolved elementary processes. The price paid by such a seemingly simpler modeling is that it is typically neither transferable nor predictive, and most importantly lacks the reverse-mapping feature much aspired in multi-scale modeling, i.e. to be able to unambiguously trace the correct microscopic origin of properties identified at the meso- or macroscopic level. All of this is possible in a theory like first-principles kMC, but one has to go the extra mile in form of an unprecedented level of detail and accuracy in the modeling. This level is at present mostly not matched in engineering-style approaches to heterogeneous catalysis, and is also the reason why existing first-principles kMC applications are hitherto still confined to well-defined model catalysts and simple reaction schemes.

D. Temperature programmed reaction spectroscopy

Properly tracking the system time kMC simulations can of course not only address catalytic systems during steady-state operation. A prominent example for a time-dependent application in the field would be temperature programmed desorption (TPD) or reaction (TPR) spectroscopies, which provide insight into the binding energetics of reaction intermediates by recording the amount of desorbing species while ramping the substrate temperature.[70] With typical experimental heating rates of a few Kelvin per second, modeling an entire TPD/TPR spectrum covering say a temperature range of a few hundred Kelvin leads again to time scales that are naturally tackled by kMC simulations. Always starting from a defined initial lattice configuration, the desorption or reaction rate as a function of temperature is there obtained from averages over an ensemble of kMC trajectories in which with progressing simulation time the temperature-dependent first-principles rate constants are adapted according to the applied heating ramp. As the kMC time does not evolve continuously, but in finite steps according to Eq. (7), there can be some technicalities with continous temperature programmes[71], which in practice can be addressed by larger simulation cells (leading to a larger $k_{\rm tot}$ and thus smaller time steps), finite temperature bins or other system-specific solutions.

Another type of TPD/TPR quantity that is typically much less sensitive to this and some other problems like slight inaccuracies in the first-principles rate constants are integral yields, i.e. the total amount of a species that has come off the surface during some extended temperature window. Such yields were e.g. measured for the $RuO_2(110)$ system from surfaces in which initially all bridge sites were always fully occupied by $O^{\rm br}$, while the coverage of $O^{\rm cus}$ varied in the range $0 < \theta < 0.8$ monolayer (ML), where 1 ML corresponds to an occupation of all cus sites.[72] The remaining free cus sites were then each time saturated with CO, so that the

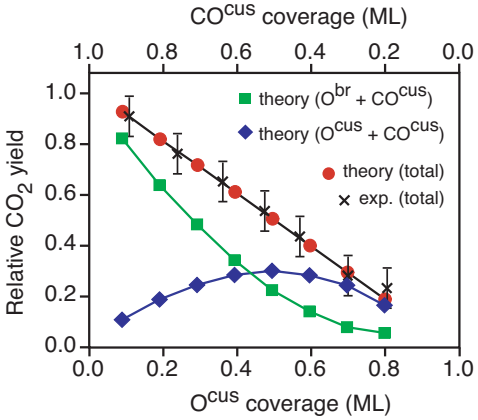

FIG. 13: Total TPR CO_2 yield from $RuO_2(110)$ surfaces initially prepared with varying O^{cus} coverage θ. In all surfaces all bridge sites are initially covered with O^{br} species, and the remaining $(1-\theta)$ cus sites not covered by O^{cus} are occupied by CO^{cus}. The CO_2 yield is given relative to the one obtained for the surface with zero O^{cus} coverage. Shown are the total simulated CO_2 yield, as well as the contributions from the two dominant reaction mechanisms under these conditions: O^{cus}+CO^{cus} and O^{br}+CO^{cus}. The experimental data is taken from ref. [72]. (From ref. [73]).

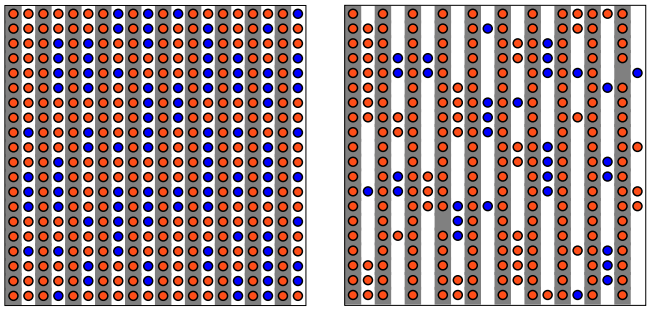

FIG. 14: Snapshots of the surface population in the first-principles TPR kMC simulation for the surface covered initially with 1 ML O^{br}, 0.5 ML O^{cus} and 0.5 ML CO^{cus}. Shown is a schematic top view as in Fig. 11, where the substrate bridge sites are marked by gray stripes and the cus sites by white stripes. Oxygen adatoms are drawn as lighter gray (red) circles and adsorbed CO molecules as darker gray (blue) circles. Left panel: Initial population at $T = 170$ K, Right panel: Population at $T = 400$ K. At this temperature, according to mean-field $> 98\,\%$ of all initially present CO^{cus} species should already have been reacted off by the low-barrier O^{cus}+CO^{cus} reaction. Instead 40% of them are still present, namely essentially all those that were not initially adsorbed immediately adjacent to a O^{cus} species. (From ref. [73]).

initially prepared surfaces contained an amount of 1 ML O^{br}, θ ML O^{cus} and $(1-\theta)$ ML CO^{cus}. The idea of this set of experiments was to evaluate which of the surface oxygen species, O^{cus} or O^{br}, is more reactive. With a constant population of O^{br} and a linearly decreasing amount of CO^{cus}, the expectation within a mean-field picture was that in case of a dominant O^{br}+CO^{cus} reaction the total CO_2 yield should show a linear $(1-\theta)$ dependence, whereas with an also linearly varying amount of O^{cus} a dominant O^{cus}+CO^{cus} reaction would be reflected by a parabolic $\theta(1-\theta)$ variation. The measured linear dependence shown in Fig. 13 was therefore taken as evidence for a much more reactive O^{br} species, which was difficult to reconcile both with the much lower DFT-GGA O^{cus} binding energy and the lower O^{cus}+CO^{cus} reaction barrier, cf. Table I.

Only subsequent first-principles kMC simulations based exactly on this DFT-GGA energetics were able to resolve this puzzle as yet another consequence of the inhomogeneities in the adlayer caused by the specific arrangement of the active sites in conjunction with diffusion limitations of the reaction intermediates.[73] As apparent from Fig. 13 the simulations perfectly reproduce the experimental data, and even reveal that the contributions from the two competing reaction channels follow indeed the functional form expected from mean-field (linear vs. parabolic). Despite the much higher O^{cus}+CO^{cus} rate constant, the share of this reaction mechanism is, however, largely suppressed as at the conditions of the TPR experiments rows of strongly bound O^{br} species confine the reactive O^{cus} species to one-dimensional cus site trenches. With strong diffusion limitations inside these trenches, cf. Table I, the CO^{cus} molecules can only access a fraction of the O^{cus} species and instead react off with their immediate O^{br} neighbors as illustrated in Fig. 14.

As also evident from Fig. 14 decreasing surface coverages toward the high-temperature end of the heating ramp are an inherent feature of TPD/TPR spectroscopy. With the concomitant increasing role of surface diffusion and a manifold of systems exhibiting rather low diffusion barriers, it is finally worth pointing out that TPD/TPR kMC simulations are particularly prone to the mentioned fastest-process bottleneck. As the gap between low and higher barrier rate constants opens up more and more with temperature, cf. Eq. (11), it is especially at the high-temperature end that the kMC algorithm increasingly ends up just executing diffusion events at minuscule time increments. Approximate workarounds to this problem include either an artificial raising of the lowest barriers or a mixing of kMC with MC schemes.[22] Both approaches work on the assumption that on the time scale of the slower processes the system essentially equilibrates over the entire subset of states that can be reached via the fast processes, i.e. that there is a separation of time scales. Raising the lowest barriers will slow down the fastest processes, which at an increased kMC efficiency will still yield an accurate dynamics if the fast processes are still able to reach equilibration even when they are slowed down. Alternatively, reducing the kMC algorithm to just the slow processes an equilibration over the subset of states reached by the fast processes can be achieved by performing some appropriate MC simulations after every

kMC step. While quite some system-specific progress has been achieved along these lines, it is in general hard to know for sure that such approximations are not corrupting the dynamics – and the low-barrier problem prevails as one of the long-standing challenges to kMC simulations.

IV. FRONTIERS

By now it has become clear that the crucial ingredients to a first-principles kMC simulation are the electronic-structure (DFT) calculations to get the PES, the mapping of this PES information onto a finite set of elementary processes and rate constants, and the master equation based kMC algorithm to evaluate the long-time evolution of the rare event system. Quite natural for a hierarchical approach spanning electronic to mesoscopic length and time scales, this reflects three complementary regimes of methodological frontiers: At the level of the electronic interactions, at the statistical-mechanics level, as well as in the interfacing in between.

Necessarily representing the finest scale in any multi-scale materials modeling, it is natural to start a short survey of open issues in the three regimes at the electronic-structure level. Obviously, if the needed accuracy is lacking at this base, there is little hope that accurate predictions can be made at any level of modeling that follows. In this respect, the accuracy level at which first-principles rate constants can presently be computed for catalytic surface systems of a complexity as the $RuO_2(110)$ example is of course a major concern. As discussed in Section II.E the limitation is thereby predominantly in the PES uncertainty, and only to a lesser extent in the prevailing use of hTST as reaction rate theory. The problem here is that approaches with an accuracy superior to the present-day workhorse DFT-GGA, but still tractable computational demand, are not readily available. This is particularly pronounced for catalytically most relevant transition metal surfaces, where post Hartree-Fock quantum chemistry methods are ill-positioned and there is increasing evidence that concomitantly also the much acclaimed hybrid DFT functionals are hardly a major step forward.[5,74] On top of this, the current focus of first-principles kMC work on the Born-Oppenheimer ground-state PES must not necessarily always convey the correct physics. Especially for core steps in the catalytic cycle like adsorption processes involving electron transfer or spin changes electronically non-adiabatic effects and the consideration of excited states may be essential.[75]

With all of these issues under active research it is crucial to realize that while a most accurate description of every elementary process is of course desirable, what matters at first in the context of first-principles kMC simulations is how the error contained in the rate constants propagates to the statistical-mechanics level and affects the resulting ensemble properties. A very promising approach is therefore to employ sensitivity analyses

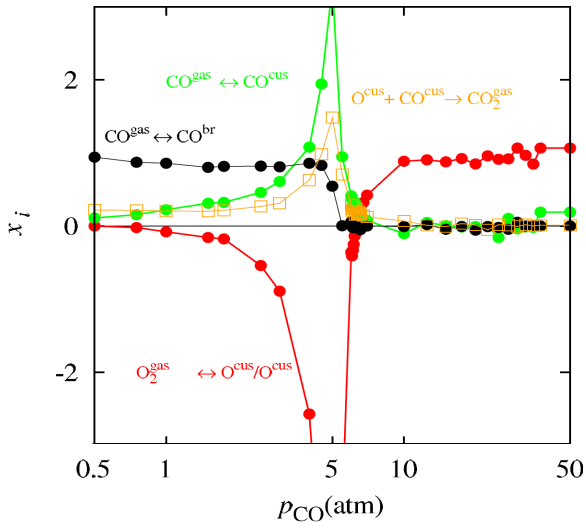

FIG. 15: Degree of rate control x_i of different elementary processes in the first-principles kMC model of CO oxidation at $RuO_2(110)$. Shown is the dependence for the gas-phase conditions of Fig. 12, where at constant $T = 600\,\mathrm{K}$ and $p_{O_2} = 1\,\mathrm{atm}$ the variation of p_{CO} causes the transition from the CO-poisoned surface state (left end of shown pressure range) to the O-poisoned surface state (right end of shown pressure range) with the catalytically most active coexistence region around $p_{CO} = 7\,\mathrm{atm}$. The DRC values for all processes not shown are zero on the scale of this figure and modest errors contained in the corresponding first-principles rate constants will practically not affect the computed TOF. (From ref. [80]).

to identify which processes critically control the targeted quantities. In the catalysis context, one possibility to identify such "rate-limiting steps" are degree of rate control (DRC) approaches, which essentially correspond to studying the linear response of the TOF to a change in one of the rate constants of the reaction network.[76–79] Such an analysis has recently been performed for the $RuO_2(110)$ system and the corresponding results for the set of gas-phase conditions also discussed in Fig. 12 are summarized in Fig. 15.[80] The most important conclusion from this work for the present discussion is that, while particularly in the catalytically most active state there is no single but an entire group of rate-limiting steps, this number of processes controlling the overall CO_2 production is small. This indicates that if the rate constants of these processes are known accurately, the kMC procedure will produce correct results even if the other rate constants are inaccurate. Strikingly, some of the unimportant rate constants could in fact be varied over several orders of magnitude with no effect on the computed TOF.[80] Apart from providing a tool for analyzing the mechanism of a complex set of catalytic reactions, such a DRC sensitivity analysis thus tells for which aspects of the reaction mechanism say a potential DFT-GGA error in the rate constants is not much of a

problem. On the other hand, it also tells which aspects must be treated accurately with corresponding errors in the rate constants directly carrying through to the mesoscopic simulation result. In this respect, the $RuO_2(110)$ DRC work revealed that under the gas-phase conditions of the experiments shown in Fig. 10 the ruling processes are the dissociative adsorption of O_2 into a cus site pair and the desorption of CO^{cus}. The almost quantitative agreement with the experimental data reached by the first-principles kMC simulations suggests therefore that especially the microscopic quantities entering the corresponding rate constants, namely the sticking coefficient of oxygen at a cus site pair and the CO^{cus} binding energy, are rather well described.[80]

At the level of the interfacing between the electronic-structure and the stochastic system description the most pressing issue is without doubt the identification of and ensuing coarse-graining to the relevant elementary processes. As most transition-state search algorithms require knowledge of the final state after the process has taken place[41,42], already quite some insight into the physics of an elementary process is needed just to determine its rate constant and include it in the list of possible kMC processes. Which processes are to be included in this list at all, and when it can be deemed complete, requires even more system-specific information. If the latter is not fully available, as is presently mostly the case, the modeler is forced to resort to chemical intuition. Unfortunately, it is by now well established that the real dynamical evolution of surface systems is full with non-obvious, unexpected and complex pathways, with surface diffusion occurring via hopping or exchange mechanisms forming a frequently cited classic example[2,81]. In this respect, the transition from MD to kMC is a paradigm for the no-free-lunch theorem: In a MD simulation the system would tell us by itself where it wants to go, yet we would be unable to follow its time evolution for a sufficiently long time. In kMC, on the other hand, the latter can be achieved, but we have to explicitly provide the possibilities where the system can go and can't be sure that we know them all.

The risk of overlooking a potentially relevant molecular process is especially consequential in first-principles kMC simulations. As discussed above, there is no possibility to cover up for a missing process as in traditional kMC simulations, where an unknown number of real molecular-level processes is in any case lumped together into a handful of effective processes with optimized rate constants. Instead, in a theory based on parameters with correct microscopic meaning such as first-principles kMC simulations omission of an important process means just one thing: A wrong result. Even if in the position of knowing all relevant processes, the problem frequently arises that with increasing system complexity this number of processes just about explodes, making a direct computation of all required rate constants from first-principles at present intractable. Examples for this are multi-site lattices or multi-species problems, or simply as already indicated in Section II.E the existence of far-reaching significant lateral interactions. And this is not to mention the degree of complications that come in if the system can not easily be mapped onto a lattice as e.g. in the case of morphological transformations of the active surface during induction or steady-state operation[82]. The technical obstacles emerging in such cases can quickly be overwhelming, and are in existing practical applications unfortunately still too often "solved" by resorting to unsystematic and unjustified approximations.

Obviously, one way out of all of these problems would be that the kMC simulation determines by itself which processes need to be considered. Imagine there is such an automatized procedure that tells which processes lead out of any given system state. Apart from solving the problem of overlooking a possibly relevant process, this also addresses the limitations imposed by an exceeding total number of processes, as one would be able to concentrate on only those processes out of states that are actually visited by the system. In principle this also supersedes the lattice approximation, unless one wants to keep it for state recognition when constructing dynamically evolving look-up tables where the information of all pathways of already visited states is kept.[83] In view of these merits, it is not surprising that such a procedure is hunted for like the holy grail. In fact, it gets reinvented over the years and features under names such as adaptive kMC[84], on-the-fly kMC[85], self-learning kMC[86] or kinetic activation-relaxation technique[87]. While the technical realizations vary, a core feature of all of these approaches is to resort to a transition-state search algorithm that only requires information about the initial state. Minimum mode following techniques like the dimer method[88,89] would be a typical example. With such an algorithm at hand, the idea is to initiate a sufficiently large number of such transition-state searches to identify all low-lying saddle points around the current state of the system (potentially accelerated MD techniques[90] could be used for this, too). The rate constant for each of these pathways is then supplied to the kMC algorithm which propagates the system in a dynamically correct way to the next state, and the procedure starts again. In principle, this is a beautiful concept that gives access to the exact time evolution, if indeed *all* bounding saddle points are found. Even if "only" the lowest-barrier escape pathways are determined, the dynamics may still be approximately ok as the omission of high-barrier pathways and their corresponding small rate constants in Eq. (5) does not introduce an exceeding error. In practice, however, it is essentially impossible to demonstrate that all (or at least all low-barrier) pathways have been found through a finite number of transition-state searches, especially for the high-dimensional PESs of systems that are of interest in catalysis research. In this situation, it is mostly a matter of taste whether one thinks that the holy grail has already been found or not. Due to the prohibitive number of first-principles energy and force evaluations required even when only employing the smallest

justifiable number of searches from each state such adaptive or on-the-fly approaches are at present in any case practically not really feasible for anything but the most trivial model systems – and on a philosophical note it is precisely those crooked PES alleys that are likely *not* to be found by a few transition-state searches that often correspond just to those nonobvious pathways that are overlooked by chemical intuition.

In examples of the type of the $RuO_2(110)$ system the computational constraints do not extend to the level of the actual kMC simulations. Compared to the costs of setting up the catalog of first-principles rate constants, running these simulations up to the required extended time spans and even for a manifold of environmental conditions represents normally an insignificant add-on, in particular as these calculations can be performed on cheaper capacity compute-infrastructures. However, this must not necessarily always be the case, and the mentioned low-barrier problem, i.e. a process operating on a much faster time scale, provides already a prototypical example where the statistical kMC simulations themselves can quickly become a bottleneck, too. This holds equally for problems with a substantially increased number of processes as often automatically implied by larger simulation cells. On a bookkeeping level significant speed-ups to overcome corresponding limitations are still realized by ever more efficient algorithms both with respect to the searches involved in the process selection step and with respect to updating the list of possible processes for a new system configuration.[20,83,91–93] Beyond this, developing concepts resort to either spatial or temporal coarse-graining, e.g. through grouping of lattice sites into coarse cells or by executing several processes at a time with approximate post-corrections of ensuing correlation errors.[20]

While the focus of such work is to improve the efficiency within the kMC framework, a more problematic issue at the general statistical-mechanics level is the Markov assumption underlying the master equation, Eq. (1). In parts, this concerns already the possibility of locally adiabatic correlated events as e.g. a sliding motion over several PES minima that are only separated by low barriers. However, if only the existence of such events is known, this kind of problem is quickly patched up by an appropriate augmentation of the list of possible kMC processes. Particularly in view of the often largely exothermic surface catalytic processes, a much more severe challenge arises instead from non-Markovian behavior resulting from a finite heat dissipation. A classic example for this would be the often controversially debated hot-adatom motion, in which after a largely exothermic dissociative adsorption process the reaction intermediate travels larger distances before it has equilibrated with the underlying substrate.[94–96] Rather than assuming a constant global temperature T as in prevailing kMC work, a consideration of such effects requires a model for the local heat transfer including e.g. an assignment of a local time-dependent temperature to each surface species accounting for its past process history.

Apart from dissipation through electronic friction and substrate phonons, a heat transfer model for steady-state catalysis at ambient pressures would furthermore need to include a heat release channel into the fluid environment. This then connects to a last frontier that actually leads outside the methodological first-principles kMC framework as sketched in this Chapter. In work of the latter type the focus is at present almost exclusively on the surface reaction chemistry, with only a rudimentary treatment of the reactive flow field over the catalyst surface. Apart from the constant global temperature mimicking an infinitely efficient heat dissipation, this concerns foremost the complete neglect of mass transfer limitations in the fluid environment as e.g. expressed by equating the reactant partial pressures entering the surface impingement, cf. Eq. (13), with those at the inlet and disregarding the built-up of a finite product concentration over the active surface as done in the described $RuO_2(110)$ work. In order to improve on this, the kMC simulations need to be adequately interfaced with a computational fluid dynamics modeling of the macro-scale flow structures in a given reactor setup.[97] While the latter are naturally described at the continuum level, the crucial difficulty is that their effects intertwine with all lower scales, with local concentration changes (or fluctuations) in the gas-phase directly and non-linearly connecting to inhomogeneities in the spatial distribution of the chemicals at the surface (e.g. reaction fronts), or the local heat dissipation at the catalyst surface intimately coupling to the kinetics and statistics of the elementary processes. The correspondingly required robust and self-consistent link of surface reaction chemistry modeling as provided by first-principles kMC with an account of the effects of heat and mass transfer as provided e.g. by time-dependent Navier-Stokes equations has to date not been achieved. In order to overcome the empirical parameters and (unscrutinized) simplifying approximations entering seminal engineering-style work tackling this coupling[98,99] will necessitate quite some further methodological developments at all involved length and time scales, but has already been identified as a core critical need in a report[100] on chemical industrial technology vision for the year 2020.

V. CONCLUSIONS

The purpose of the present Chapter was to introduce the first-principles kinetic Monte Carlo approach in its specific flavor geared toward heterogeneous catalytic applications, as well as to provide an impression of its present capabilities and open frontiers. As a hierarchical approach, first-principles kMC jointly addresses two complementary and crucial aspects of reactive surface chemistry, namely an accurate description of the elementary processes together with a proper evaluation of their statistical interplay. For the prior it resorts to first-

principles electronic structure theories, for the latter to a master equation based description tackling the rare event evolution of surface catalytic systems. The result is a powerful technique that gives access to the surface chemical kinetics at an unprecedented accuracy, in particular by including a sound quantum-mechanical description of the ubiquitous bond making and breaking and by including a full account of the atomic-scale correlations, fluctuations, and spatial distributions of the chemicals at the active surface sites. As a technique based on elementary processes with a clear-cut microscopic meaning, first-principles kMC is naturally transferable and can provide comprehensive insight into the on-going surface chemistry over a wide range of temperature and pressure conditions.

In its philosophy, it is clearly a bottom-up approach that aims to propagate the predictive power of first-principles techniques up to increasing length and time scales. For this it is important to realize that at both the electronic structure and the statistical-mechanics level the various applied approximations introduce uncertainty, and the bridging from one scale to the other gives rise to additional uncertainty. With such multiple sources of uncertainty affecting the final result, only a stringent error control will ever allow to assign the desired predictive quality to the simulation. Most pressing issues for such a robust link at the transition between the molecular and mesoscopic scale are presently the identification of and ensuing coarse-graining to the relevant elementary processes, as well as the propagation of error in the first-principles rate constants to the ensemble properties resulting from the statistical interplay.

With the stated claim of predictive quality first-principles kMC simulations inherently require a level of detail and effort that is uncommon, if not far beyond standard effective modeling based on empirical parameters. Critical issues here are the necessity of a well-established microscopic characterization of the active surface sites, as well as the computational cost to determine accurate first-principles rate constants for a number of elementary processes that virtually explodes with increasing system complexity. As a result, existing practical applications are still restricted to single-crystal model catalysts and reaction schemes of modest complexity, but this will undoubtedly change with further algorithmic developments and ever increasing computational power. The demanding characteristics of the approach must also be born in mind when attempting the now due interfacing of first-principles kMC with their focus on the surface chemistry with macroscopic theories that model the heat and mass transport in the system, i.e. the flow of chemicals over the catalyst surface and the propagation of the heat released during the on-going chemical reactions.

Corresponding developments will necessitate incisive methodological advances at all involved length and time scales, and have to overcome the present standard of uncontrolled semi-empiricism and effective treatments. Yet, they are fired by the imagination of an ensuing error-controlled multi-scale modeling approach which starting from the molecular-level properties will yield a quantitative account of the catalytic activity over the entire relevant range of reactive environments. Most importantly, this also encompasses a full "reverse mapping" capability to the mechanistic aspects, i.e. the power to analyze in detail how the electronic-structure (bond breaking and bond making) actuates the resulting macroscopic catalytic properties, function and performance. I am convinced that it is ultimately only the concomitant new level of understanding that will pave the way for a rational design of tailored material-, energy- and cost-efficient catalysts, and it is this vision that makes working on these problems so exciting and worthwhile.

VI. ACKNOWLEDGEMENTS

I began using kinetic Monte Carlo simulations to model surface catalytic problems some 5-6 years ago. During this entire time I have been working at the Fritz-Haber-Institut, and much of the progress and understanding reviewed in this Chapter would have been impossible without the enlightening and stimulating environment offered by this unique institution. In this respect it is a pleasure to gratefully acknowledge the countless discussions with all members of the Theory Department that ultimately led to the specific vision of the first-principles kMC approach described here. This holds prominently and foremost for Matthias Scheffler, with whom most of the work on the $RuO_2(110)$ system was carried out.

---

[1] *Handbook of Materials Modeling*, S. Yip (Ed.), Springer, Berlin (2005).

[2] K. Reuter, C. Stampfl, and M. Scheffler, *Ab initio Atomistic Thermodynamics and Statistical Mechanics of Surface Properties and Functions*, in Handbook of Materials Modeling, Vol. 1, p. 149-194, S. Yip (Ed.), Springer, Berlin (2005).

[3] C.J. Kramer, *Essentials of Computational Chemistry: Theories and Models*, 2nd edn., Wiley, Chichester (2004).

[4] R.M. Martin, *Electronic-Structure: Basic Theory and Practical Methods*, Cambridge University Press, Cambridge (2004).

[5] E.A. Carter, Science **321**, 800 (2008).

[6] N.G. van Kampen, *Stochastic Processes in Physics and Chemistry*, North-Holland Publishing, Amsterdam (1980).

[7] D. Chandler, *Introduction to Modern Statistical Mechanics*, Oxford University Press, Oxford (1987).

[8] Another less frequently employed name for kinetic Monte Carlo is dynamic Monte Carlo, with all of the early con-

ceptual papers typically just referring to Monte Carlo. See e.g. the excellent review by Voter[9] for a nice account of the historic development of this technique.

[9] A.F. Voter, *Introduction to the Kinetic Monte Carlo Method*, in Radiation Effects in Solids, K.E. Sickafus, E.A. Kotomin and B.P. Uberuaga (Eds.), Springer, Berlin (2007).

[10] R.I. Masel, *Principles of Adsorption and Reaction on Solid Surfaces*, Wiley, New York (1996).

[11] R.I. Masel, *Chemical Kinetics and Catalysis*, Wiley, New York (2001).

[12] I. Chorkendorff and J.W. Niemantsverdriet, *Concepts of Modern Catalysis and Kinetics*, Wiley-VCH, Weinheim (2003).

[13] D.J. Wales, *Energy Landscapes*, Cambridge University Press, Cambridge (2003).

[14] D. Frenkel and B. Smit, *Understanding Molecular Simulation*, 2nd edn., Academic Press, San Diego (2002).

[15] D.P. Landau and K. Binder, *A Guide to Monte Carlo Simulations in Statistical Physics*, Cambridge University Press, Cambridge (2002).

[16] D.T. Gillespie, J. Comp. Phys. **22**, 403 (1976).

[17] K.A. Fichthorn and W.H. Weinberg, J. Chem. Phys. **95**, 1090 (1991).

[18] D.T. Gillespie, J. Phys. Chem. **81**, 2340 (1977).

[19] J.G. Amar, Computing in Science and Engineering **8**, 9 (2006).

[20] A. Chatterjee and D.G. Vlachos, J. Computer-Aided Mater. Design **14**, 253 (2007).

[21] A.B. Bortz, M.H. Kalos, and J.L. Lebowitz, J. Comp. Phys. **17**, 10 (1975).

[22] H.C. Kang and W.H. Weinberg, Chem. Rev. **95**, 667 (1995).

[23] N. Metropolis, A.W. Rosenbluth, M.N. Rosenbluth, A.H. Teller, and E. Teller, J. Chem. Phys. **21**, 1087 (1953).

[24] K. Kawasaki, in *Phase Transitions and Critical Phenomena*, C. Domb and M. Green (Eds.), Academic Press, London (1972).

[25] E. Wigner, Z. Phys. Chem. B **19**, 203 (1932).

[26] H. Eyring, J. Chem. Phys. **3**, 107 (1935).

[27] P. Haenggi, P. Talkner, and M. Borkovec, Rev. Mod. Phys. **62**, 251 (1990).

[28] G.H. Vineyard, J. Phys. Chem. Solids **3**, 121 (1957).

[29] K. Reuter, D. Frenkel, and M. Scheffler, Phys. Rev. Lett. **93**, 116105 (2004); K. Reuter and M. Scheffler, Phys. Rev. B **73**, 045433 (2006).

[30] C. Dellago, P.G. Bolhuis, and P.L Geissler, Adv. Chem. Phys. **123**, 1 (2002).

[31] B.C. Garrett and D.G. Truhlar, *Variational Transition State Theory*, in Theory and Applications in Computational Chemistry: The First Forty Years, p. 67-87, C. Dykstra, G. Frenking, K. Kim, and G. Scuseria (Eds.), Elsevier, Amsterdam (2005).

[32] R.G. Parr and W. Yang, *Density Functional Theory of Atoms and Molecules*, Oxford University Press, Oxford (1989).

[33] R.M. Dreizler and E.K.U. Gross, *Density Functional Theory*, Springer, Berlin (1990).

[34] W. Koch and M.C. Holthausen, *A Chemist's Guide to Density Functional Theory*, 2nd edn., Wiley-VCH, Weinheim (2001).

[35] J.P. Perdew and K. Schmidt, in *Density Functional Theory and Its Application to Materials*, V. Van Doren, C. Van Alsenoy, and P. Geerlings (Eds.), American Institute of Physics, Melville (2001).

[36] A.J. Cohen, P. Mori-Sanchez, and W. Yang, Nature **321**, 792 (2008).

[37] M. Scheffler and C. Stampfl, *Theory of Adsorption on Metal Substrates*, in Handbook of Surface Science. Vol 2: Electronic Structure, K. Horn and M. Scheffler (Eds.), Elsevier, Amsterdam (2000).

[38] A. Groß, *Theoretical Surface Science A Microscopic Perspective*, Springer, Berlin (2002).

[39] M.C. Payne, M.P. Teter, D.C. Allan, T.A. Arias, and J.D. Joannopoulos, Rev. Mod. Phys. **64**, 1045 (1992).

[40] G. Henkelman, G. Johannesson, and H. Jonsson, *Methods for Finding Saddle Points and Minimum Energy Paths*, in Progress on Theoretical Chemistry and Physics, S.D. Schwarz (Ed.), Kluwer, New York (2000).

[41] H.P. Hratchian and H.B. Schlegel, *Finding Minima, Transition States and Following Reaction Pathways on ab initio Potential Energy Surfaces*, in Theory and Applications in Computational Chemistry: The First Forty Years, p. 195-250, C. Dykstra, G. Frenking, K. Kim, and G. Scuseria (Eds.), Elsevier, Amsterdam (2005).

[42] H. Jonsson, G. Mills, and K.W. Jacobson, *Nudged Elastic Band Method for Finding Minimum Energy Paths of Transitions*, in Classical and Quantum Dynamics in Condensed Phase Simulations, B.J. Berne, G. Cicotti, and D.F. Coker (Eds.), World Scientific, New Jersey (1998).

[43] G. Henkelman, B.P. Uberuaga, and H. Jonsson, J. Chem. Phys. **113**, 9901 (2000).

[44] A.F. Voter, Phys. Rev. B **34**, 6819 (1986).

[45] K.A. Fichthorn and M. Scheffler, Phys. Rev. Lett. **84**, 5371 (2000); K.A. Fichthorn, M.L. Merrick, and M. Scheffler, Appl. Phys. A **75**, 17 (2002).

[46] J.M. Sanchez, F. Ducastelle, and D. Gratias, Physica A **128**, 334 (1984).

[47] D. De Fontaine, in Statics and Dynamics of Alloy Phase Transformations, P.E.A. Turchy and A. Gonis (Eds.), NATO ASI Series, Plenum Press, New York (1994).

[48] A. Zunger, *First Principles Statistical Mechanics of Semiconductor Alloys and Intermetallic Compounds*, in Statics and Dynamics of Alloy Phase Transformations, P.E.A. Turchy and A. Gonis (Eds.), NATO ASI Series, Plenum Press, New York (1994).

[49] C. Stampfl, H.J. Kreuzer, S.H. Payne, H. Pfnür, and M. Scheffler, Phys. Rev. Lett. **83**, 2993 (1999).

[50] R. Drautz, R. Singer, and M. Fähnle, Phys. Rev. B **67**, 035418 (2003).

[51] H. Tang, A. van der Ven, and B.L. Trout, Phys. Rev. B **70**, 045420 (2004); Mol. Phys. **102**, 273 (2004).

[52] M. Fähnle, R. Drautz, F. Lechermann, R. Singer, A. Diaz-Ortiz, and H. Dosch, phys. stat. sol. (b) **242**, 1159 (2005).

[53] Y. Zhang, V. Blum, and K. Reuter, Phys. Rev. B **75**, 235406 (2007).

[54] E.W. Hansen and M. Neurock, Chem. Eng. Sci. **54**, 3411 (1999).

[55] E. Shustorovich and H. Sellers, Surf. Sci. Rep. **31**, 5 (1998).

[56] P. Ruggerone, C. Ratsch, and M. Scheffler, *Density-Functional Theory of Epitaxial Growth of Metals*, in Growth and Properties of Ultrathin Epitaxial Layers, D.A. King and D.P. Woodruff (Eds.), The Chemical Physics of Solid Surfaces Vol. **8**, Elsevier, Amsterdam (1997).

[57] P. Kratzer, E. Penev, and M. Scheffler, Appl. Phys. A **75**, 79 (2002).

[58] K. Reuter, Oil& Gas Sci. and Technol. - Rev. IFP **61**, 471 (2006).
[59] H. Over and M. Muhler, Prog. Surf. Sci. **72**, 3 (2003).
[60] K. Reuter and M. Scheffler, Phys. Rev. B **68**, 045407 (2003).
[61] N. Brønsted, Chem. Rev. **5**, 231 (1928); M.G. Evans and N.P. Polanyi, Trans. Faraday Soc. **32**, 1333 (1936).
[62] B. Temel, H. Meskine, K. Reuter, M. Scheffler, and H. Metiu, J. Chem. Phys. **126**, 204711 (2007).
[63] V.P. Zhdanov and B. Kasemo, Surf. Sci. Rep. **20**, 111 (1994).
[64] R.M. Ziff, E. Gulari, and Y. Barshad, Phys. Rev. Lett. **56**, 2553 (1986); B.J. Brosilow and R.M. Ziff, Phys. Rev. A **46**, 4534 (1992).
[65] P.I. Stoltze, Prog. Surf. Sci. **65**, 65 (2000).
[66] K. Reuter and M. Scheffler, Phys. Rev. Lett. **90**, 046103 (2003).
[67] K. Reuter and M. Scheffler, Appl. Phys. A **78**, 793 (2004).
[68] J. Wang, C.Y. Fan, K. Jacobi, and G. Ertl, J. Phys. Chem. B **106**, 3422 (2002).
[69] S. Matera, unpublished results.
[70] D.P. Woodruff and T.A. Delchar, *Modern Techniques of Surface Science*, Cambridge Univ. Press, Cambridge (1994).
[71] A.P.J. Jansen, Comp. Phys. Commun. **86**, 1 (1995).
[72] S. Wendt, M. Knapp, and H. Over, J. Am. Chem. Soc. **126**, 1537 (2004).
[73] M. Rieger, J. Rogal, and K. Reuter, Phys. Rev. Lett. **100**, 016105 (2008).
[74] A. Stroppa and G. Kresse, New J. Phys. **10**, 063020 (2008).
[75] G.-J. Kroes, Science **321**, 794 (2008).
[76] M. Boudard and K. Tamaru, Catal. Lett. **9**, 15 (1991).
[77] C.T. Campbell, Topics Catal. **1**, 353 (1994).
[78] J.A. Dumesic, J. Catal. **185**, 496 (1999).
[79] A. Baranski, Solid State Ionics **117**, 123 (1999).
[80] H. Meskine, S. Matera, M. Scheffler, K. Reuter, and H. Metiu, Surf. Sci. (*in press*).
[81] T. Ala-Nissila, R. Ferrando, and S.C. Ying, Adv. Phys. **51**, 949 (2002).
[82] see e.g. the discussion in J. Rogal, K. Reuter, and M. Scheffler, Phys. Rev. Lett. **98**, 046101 (2007); Phys. Rev. B **77**, 155410 (2008).
[83] D.R. Mason, T.S. Hudson, and A.P. Sutton, Comp. Phys. Commun. **165**, 37 (2005).
[84] G. Henkelman and H. Jonsson, J. Chem. Phys. **115**, 9657 (2001).
[85] J.L. Bocquet, Defect Diffus. Forum **203**, 81 (2002).
[86] O. Trushin, A. Karim, A. Kara, and T.S. Rahman, Phys. Rev. B **72**, 115401 (2005).
[87] F. El-Mellouhi, N. Mousseau, and L.J. Lewis, Phys. Rev. B **78**, 153202 (2008).
[88] G. Henkelman and H. Jonsson, J. Chem. Phys. **111**, 7010 (1999).
[89] A. Heyden, A.T. Bell, and F.J. Keil, J. Chem. Phys. **123**, 224101 (2005).
[90] A.F. Voter, F. Montalenti, and T.C. Germann, Annu. Rev. Mater. Res. **32**, 321 (2002).
[91] J.L. Blue, I. Beichl, and F. Sullivan, Phys. Rev. E **51**, R867 (1994).
[92] M.A. Gibson and J. Bruck, J. Phys. Chem. A **104**, 1876 (2000).
[93] T.P. Schulze, Phys. Rev. E **65**, 036704 (2002).
[94] H. Brune, J. Wintterlin, R.J. Behm, and G. Ertl, Phys. Rev. Lett. **68**, 624 (1992).
[95] J. Wintterlin, R. Schuster, and G. Ertl, Phys. Rev. Lett. **77**, 123 (1996).
[96] S. Schintke, S. Messerli, K. Morgenstern, J. Nieminen, and W.-D. Schneider, J. Chem. Phys. **114**, 4206 (2001).
[97] O. Deutschmann, *Computational Fluid Dynamics Simulation of Catalytic Reactors*, p. 1811-1828, Chapter 6.6 in Handbook of Heterogeneous Catalysis, 2nd Ed., G. Ertl, H. Knzinger, F. Schth, and J. Weitkamp (eds.), Wiley-VCH, Weinheim (2008).
[98] R. Kissel-Osterrieder, F. Behrendt, J. Warnatz, U. Metka, H.R. Volpp, and J. Wolfrum, Proc. of the Combustion Institute **28**, 1341 (2000).
[99] D.G. Vlachos, A.B. Mhadeshwar, and N.S. Kaisare, Computers & Chemical Engineering **30**, 1712 (2006).
[100] Technology Vision 2020: The U.S. Chemical Industry, American Chemical Society, American Institute of Chemical Engineers, The Chemical Manufactures Association, The Council for Chemical Research, and The Synthetic Organic Chemical Manufactures (1996). http://www.ccrhq.org/vision/welcome.html